Drivers and vertical CO_2 flux balances in a Sahelian agroforestry system: Insights from high frequency measurements

Seydina Mohamad Ba [a d], Olivier Roupsard [b c d], Lydie Chapuis-Lardy [c f], Frédéric Bouvery [g], Yélognissè Agbohessou [h i j], Maxime Duthoit [c e], Aleksander Wieckowski [k], Torbern Tagesson [k], Mohamed Habibou Assouma [l], Espoir K. Gaglo [a d], Claire Delon [m], Bienvenu Sambou [a], Dominique Serça [m]

[a] Faculté des Sciences et Techniques (FST), Institut des Sciences de l'Environnement (ISE), Université Cheikh Anta Diop (UCAD) de Dakar, 5005, Dakar-Fann, Sénégal

[b] CIRAD, UMR Eco&Sols, Dakar, Sénégal

[c] Eco&Sols, Univ Montpellier, CIRAD, INRAE, Institut Agro, IRD, Montpellier, France

[d] LMI IESOL, Centre IRD-ISRA de Bel Air, Route des hydrocarbures, 18524, Dakar, Sénégal

[e] CIRAD, UMR Eco&Sols, Université de Montpellier, Cirad, INRAE, IRD, Institut Agro Montpellier, 2 place Viala, Montpellier, France

[f] IRD, UMR Eco&Sols, Université de Montpellier, Cirad, INRAE, IRD, Institut Agro Montpellier, 2 place Viala, Montpellier, France

[g] INRAE, 147 rue de l'Université, 75338 Paris, France

[h] AIDA, Univ Montpellier, CIRAD, Montpellier, France

[i] CIRAD, UPR AIDA, Harare, Zimbabwe

[j] Department of Plant Production Sciences and Technologies, University of Zimbabwe, Harare, Zimbabwe

[k] Department of Physical Geography and Ecosystem Science, Lund University, Sölvegatan 12, S-223 62 Lund, Sweden

[l] UMR SELMET, CIRAD, INRAE, Univ Montpellier, Institut SupAgro, Montpellier, France

[m] Laboratoire d'Aérologie, Université de Toulouse, CNRS, IRD, 14 Avenue Edouard Belin, 31400 Toulouse, France

Corresponding authors:
Seydina Mohamad Ba: seydina.ba@ird.fr
Olivier Roupsard: olivier.roupsard@cirad.fr

Highlights:

- Long-term high frequency CO_2 flux measurements using automated dynamic chambers in a Sahelian *F. albida* parkland.
- Empirical gap-filling and flux partitioning methods validated against Eddy Covariance GPP.
- Fluxes peaked during the rainy season both at a distance from trees in full sun (FS) and under tree canopies (Sh), driven mainly by soil moisture and leaf area.
- *F. albida* trees enhance CO_2 fluxes under canopies ("fertile island" effect) and account for ~23% of annual ecosystem GPP.

ABSTRACT:

Agroforestry systems — combining trees with crops and/or livestock — are increasingly promoted as sustainable and climate-resilient land-use strategies. Despite their widespread presence in the Sahel, experimental data on their potential as carbon sinks are scarce. This study presents a full-year, high-frequency dataset of CO_2 fluxes in a Sahelian agro-silvo-pastoral parkland dominated by *Faidherbia albida*, located in Senegal's groundnut basin. CO_2 fluxes were continuously measured using automated dynamic chambers, allowing the quantification of soil and crop respiration (Rch), gross primary production (GPPch), and net carbon exchange (FCO_2ch) under both full sun and shaded (under tree canopies) environments. Seasonal patterns of CO_2 fluxes were similar in both environments, with peaks during the rainy season. Rch and GPPch were significantly higher under tree canopies, indicating a 'fertile island' effect. CO_2 flux variability was primarily driven by soil moisture and leaf area index. Chamber-based GPP estimates closely matched those from Eddy Covariance measurements. On an annual scale, *F. albida* trees contributed approximately 23% of total ecosystem GPP, with a carbon use efficiency of 0.48. Net annual vertical CO_2 exchange was estimated at -1.4 ± 0.46 and -1.8 ± 0.17 Mg C-CO_2 ha^{-1} using chamber and Eddy Covariance methods, respectively. These findings underscore the role of *F. albida*-based agroforestry systems as effective carbon sinks in Sahelian landscapes, supporting their potential contribution to climate change mitigation.

Keywords: Sahelian agro-silvo-pastoral systems, CO_2 fluxes, automated dynamic chambers, Eddy Covariance, 'fertile island effect', carbon balances.

1. Introduction

Plant photosynthesis and respiration —both autotrophic (plant) and heterotrophic (microbial)— are fundamental processes driving carbon dioxide (CO_2) fluxes in terrestrial ecosystems (Lambers et al., 2008; Raich et al., 2014; Reichle, 2020). Accurate quantification of these processes is critical for assessing ecosystem carbon (C) sink potential (Baldocchi, 2020), particularly for informing climate-smart land management strategies.

To capture these processes at the ecosystem scale, the Eddy Covariance (EC) technique has emerged as a transformative method, enabling continuous and high-frequency CO_2 flux measurements (Baldocchi, 2003, 2008). The EC technique quantifies CO_2 exchanges between ecosystems and the atmosphere by correlating fluctuations in vertical wind velocity with simultaneous variations in CO_2 concentrations, providing a direct and non-invasive estimate of CO_2 fluxes (Baldocchi, 2003). Extensive EC networks in Europe (Stojanović et al., 2024), Asia (Yu et al., 2011), and the Americas (Chu et al., 2021) have significantly advanced our understanding of the global C cycle. In contrast, sub-Saharan Africa remains critically underrepresented (Bombelli et al., 2009; Houghton & Hackler, 2006; Williams et al., 2007). Although some studies have used EC (Ardö et al., 2008; Brümmer et al., 2008; Merbold et al., 2009; Tagesson et al., 2016), static chambers (Assouma et al., 2017; Owusu et al., 2024; Rosenstock et al., 2016; Wachiye et al., 2020), or modeling approaches (Agbohessou et al., 2023, 2024; Delon et al., 2019; Rahimi et al., 2021), they remain sparse and methodologically heterogeneous, limiting comparability and regional C budget integration.

Among these underrepresented landscapes, agroforestry systems in the Sahel— particularly agro-silvo-pastoral systems (ASPS) that combine trees, crops, and livestock— are increasingly promoted for sustainable land management and climate resilience (Cardinael et al., 2021; Gupta et al., 2023; Mbow et al., 2014; Stetter & Sauer, 2024). However, the structural and functional heterogeneity of these systems poses significant challenges for accurately quantifying and upscaling C fluxes. *Faidherbia albida*, a keystone agroforestry tree species in these ASPS (Leroux et al., 2022; Lu et al., 2022), is of particular interest due to its reverse phenology, capacity to enhance soil fertility and crop yields (Bayala et al., 2020; Roupsard et al., 2020; Sileshi et al., 2016; 2020). Yet, its functional role in modulating both the magnitude and seasonal dynamics of CO_2 fluxes remains poorly understood.

Addressing this knowledge gap requires integrated approaches capable of capturing both aggregate and component-specific CO_2 fluxes. While EC remains the gold standard method for CO_2 flux measurements at the landscape scale (Baldocchi, 2003), it captures net ecosystem exchange (NEE) as an aggregate signal, without separating the contributions from individual compartments such as soil, crops, and trees. This limits its utility for disentangling processes and attributing sources in heterogeneous systems like ASPS. Automated dynamic chambers provide a valuable

complement to EC, as they enable continuous, high-frequency measurements at finer scales and at the level of specific ecosystem components. This approach facilitates component-specific quantification of CO_2 fluxes, particularly from soil and crop compartments (Luo & Zhou, 2006; Denmead, 2008; Zaman et al., 2021). When combined with EC, this dual-method approach strengthens source attribution and improves the partitioning of fluxes across complex agroforestry landscapes.

This study presents one of the first integrated quantification of CO_2 fluxes in a Sahelian ASPS dominated by *F. albida*, combining EC and automated dynamic chambers.

Specifically, the study aims to (1) conduct year-round, high-frequency *in situ* CO_2 flux measurements from soil and crops using automated dynamic chambers; (2) partition the net CO_2 fluxes (FCO_2ch) into respiration (Rch) and photosynthesis (GPPch); (3) investigate the environmental drivers of fluxes and the spatial variability linked to tree presence; and (4) compare chamber-based flux estimates with ecosystem-scale measurements derived from the EC method.

Based on these objectives, we hypothesize that (1) Rch and GPPch are higher under the canopy of *F. albida* than in full sun, (2) soil moisture is the main environmental factor directly controlling both Rch and GPPch, (3) when extrapolated to the field scale, the chamber-based method provides seasonal dynamics of respiration and photosynthesis fluxes comparable to those derived from EC technique.

2. Materials and methods

2.1. Site description

The study was conducted in the agroforestry parkland of Sob village (Niakhar municipality, Fatick region), located in the groundnut basin of Senegal, within the Sahelo-Sudanian climatic zone of West Africa (Fig. 1). The climate is characterized by a long dry season (8–9 months) with high temperatures and strong diurnal variations, and a short rainy season from late June to mid-October (Delaunay et al., 2018).

Soils are locally known as "*Dior"* and classified as Arenosols (IUSS Working Group WRB, 2022). The topsoil has low organic matter (<1%) and phosphorus (<3 mg kg^{-1}), a sandy texture (>85% sand), and an acidic pH (Malou et al., 2021; Siegwart et al., 2022). Rainfed agriculture predominates. The main cropping system includes pearl millet (*Pennisetum glaucum L.*) and groundnut (*Arachis hypogaea L.*) in biennial rotation, with occasional intercropping of cowpea (*Vigna unguiculata L.*).

The site hosts the 'Faidherbia Flux' station (14°29′44.916″N; 16°27′12.851″W; FLUXNET ID: SN-Nkr), a long-term research platform for monitoring ecosystem services in agroforestry systems. It is dominated by *F. albida*, a nitrogen-fixing, reverse-phenology tree with deep roots accessing groundwater (Roupsard et al., 1999). The tree density is ~13 trees ha^{-1}, with canopies covering ~10% of the soil surface (Roupsard et al., 2020). The EC tower is installed at 20 m height, approximately 12.5 m above the canopy. The study field is a typical 'bush field', characterized by low soil fertility, no mineral fertilization, and off-site export of crop residues and manure (Malou et al., 2021).

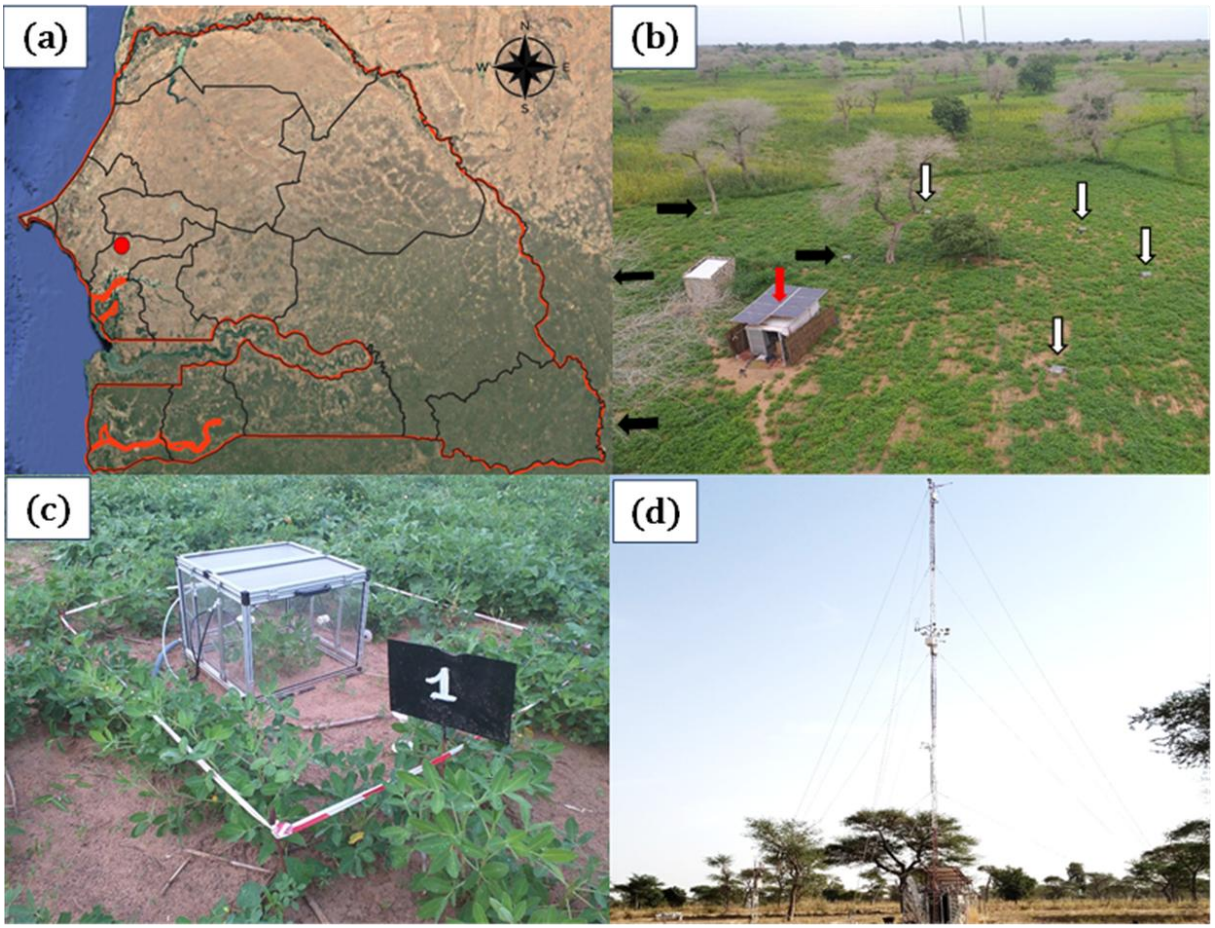

Fig. 1: Study area.

(a) geographical location of Sob, Groundnut basin, Senegal (Map data © Google Earth, 2025), (b) overview (image from the Eddy Covariance tower located in the same bush-field) of the *Faidherbia albida* parkland during the rainy season, depicting groundnut crops with bare soil in the inter-row, *F. albida* trees (defoliated during the rainy season, average height = 13m) and location of the chambers under the Shade of trees (horizontal black arrows; N=4) and in Full sun (vertical white arrows; N=4); The shelter (red arrow) with solar panels is to fit the analyser, automation and batteries (c) automatic chamber enclosing a groundnut plant (during the rainy season) or bare soil (during the dry season), (d) Eddy Covariance (EC) tower (measurement height = 20 m) during the dry season.

2.2. Experimental setup

2.2.1. CO_2 flux measurements in automatic chambers

Continuous net CO_2 fluxes (FCO_2ch) from soil and groundnut plants were measured over a full phenological year (June 17, 2021 – June 17, 2022) using eight automated dynamic chambers (50×50×50 cm), each enclosing one groundnut plant. Four chambers were installed in full sun (FS), at least 20 m from trees, and four under *F. albida* canopy shade (Sh). The chambers were transparent, custom-built (Duthoit et al., 2020), and installed on metal bases embedded 10 cm into the soil one month prior to measurements.

During the rainy season (June–November), groundnut coexisted briefly with spontaneous weeds until weeding (mid-July), after which chambers contained only groundnut. Post-harvest (early November), chambers remained bare while surrounding plots experienced weed regrowth.

CO_2 concentrations were measured at 1 Hz using a Picarro G2508 gas analyser (Picarro Inc., Santa Clara, CA, USA) (Fleck et al., 2013; Reum et al., 2019; Valujeva et al., 2022). A fully automated system was built for sequential half-hour flux measurements alternating FS and Sh chambers (Table S2). Measurement duration was 15 min per chamber in the dry season, reduced to 5 min during the rainy season to limit condensation effects.

2.2.2. CO_2 flux measurements by Eddy Covariance

The EC system (Li-COR SMARTFLUX®, including a Gill MasterPro 3D sonic anemometer and a LI-7500 RS open path CO_2 and H_2O gas analyser) was mounted at a height of 20 m on a 30m mast, above *F. albida*. It continuously monitored net CO_2 exchange from the ecosystem. Raw data were collected at 20 Hz frequency and post-processed from binary files using the advanced mode of the EddyPro® v7.0, with standard corrections and procedures: sonic tilt correction (double rotation), block averaging, covariance maximisation for time lag, and WPL correction (Webb et al., 1980). Quality control followed Foken et al. (2004) and Vickers & Mahrt (1997); random uncertainty was estimated per Finkelstein & Sims (2001). Spectral corrections were applied according to Moncrieff et al. (1997, 2004). Footprints were computed according to Kormann and Meixner (2001), using the FREddyPro R package (Xenakis, 2016), indicating a ~1 ha source area covering the entire field. Gap-filling and flux partitioning were conducted using ReddyProc (Wutzler et al., 2018), applying the daytime partitioning approach of Lasslop et al. (2010).

2.2.3. Ancillary measurements

Environmental and vegetation variables were monitored continuously throughout the study. Global radiation (Rg) was estimated from photosynthetically active radiation (PAR) using a Skye sensor (averaged over 30-min intervals). The normalised difference vegetation index (NDVI) of

crops under full sun was recorded semi-hourly by a calibrated downward-facing sensor installed at 20 m height (Pontailler et al., 2003), processed following Soudani et al. (2012), and used to estimate the leaf area index (LAI) time series for groundnut, weeds, and cowpea based on end-of-season field LAI measurements in six 15 m^2 plots (as in Roupsard et al., 2020).

Rainfall was recorded by an automatic weather station (CR1000 with TE525MM rain gauge, Campbell Scientific), and soil volumetric water content (VWC) and temperature (T_{soil}, at 6 cm depth) were monitored using TOMST® TMS-4 sensors, benchmarked prior to field deployment inside and outside the chambers (Wild et al., 2019). Air temperature (T_{air}) was recorded inside each chamber at 15 cm above ground, all at 5-min intervals. These measurements contribute to the SoilTemp global database (Lembrechts et al., 2020, 2022).

Groundnut development was tracked weekly by counting leaves in each chamber. Total groundnut LAI (LAIch) was then derived from average single-leaf area and chamber surface.

A detailed description of the data used in this study is provided in Supplement (Table S1).

2.3. Data processing

2.3.1. Flux calculation

Net CO_2 fluxes (FCO_2ch, in µmol CO_2 m^{-2} s^{-1}) from the chambers were calculated from the linear change in CO_2 concentration over time ($\Delta C/\Delta t$; Fig. S1 and Fig. S2) using the Eq.1.

$$\mathbf{FCO_2ch} = \left(\frac{\mathbf{P}}{\mathbf{RTk}}\right)\left(\frac{\mathbf{V}}{\mathbf{A}}\right)\left(\frac{\mathbf{\Delta C}}{\mathbf{\Delta t}}\right) \qquad \textbf{(Eq. 1)}$$

where P is atmospheric pressure (101 325 N m^{-2}), R is the ideal gas constant (8.31 N m mol^{-1} K^{-1}), T_k is air temperature inside the chamber in Kelvin, V (0.125 m^3) is the total system volume (chamber, tubing, analyser cavity, pump, and water trap), and A (0.25 m^2) is the chamber footprint. The slope $\Delta C/\Delta t$ was obtained via linear regression (Duthoit et al., 2020).

Mean FCO_2ch values were computed separately for the four replicate chambers in full sun (FS) and under *F. albida* shade (Sh). By convention, negative values indicate net CO_2 uptake (photosynthesis), and positive values indicate net CO_2 release (respiration).

2.3.2. Quality control of chamber-based CO_2 flux measurements

The quality of chamber-based CO_2 flux measurements was assessed using a threshold of $R^2 \geq 0.8$ of the linear increase in CO_2 concentration during chamber closure. The minimum detectable flux (MDF) was then calculated following Nickerson (2016) (Eq.2). The MDF defines the flux detection threshold, below which data are considered unreliable due to instrument sensitivity and sampling constraints (Zaman et al., 2021). In this study, the MDF was ± 0.0004 µmol CO_2 m^{-2} s^{-1}.

$$\mathbf{MDF} = \left(\frac{\mathbf{Aa}}{\mathbf{tc}\left(\sqrt{\mathbf{tc}/\mathbf{ps}}\right)}\right)\left(\frac{\mathbf{VP}}{\mathbf{ART}}\right) \quad \textbf{(Eq. 2)}$$

where A_a is the analytical precision of the Picarro analyser (0.6 ppm; Picarro Inc., 2015), tc the closure time (s), p_s the sampling frequency (1 Hz), V the chamber volume, P the atmospheric pressure (101 325 N m^{-2}), A the chamber footprint, R the gas constant (8.3 N m $mol^{-1} \cdot K^{-1}$), and T the air temperature in Kelvin.

Following this quality control, fluxes were partitioned (Section 2.3.3) and gap-filled (Section 2.3.4).

2.3.3. Partitioning of chamber-based CO_2 fluxes

The net CO_2 fluxes (FCO_2ch), averaged from four chambers per environment (FS and Sh), were partitioned into two components according to Eq. 3 (Reichstein et al., 2005).

$$\mathbf{FCO_2ch} = \mathbf{Rch} + \mathbf{GPPch} \quad \textbf{(Eq. 3)}$$

Rch includes heterotrophic respiration (Rh) from soil and other autotrophic respiration (Ra) from groundnut plants and roots of *F. albida* (Ra Groundnut + Ra tree below-ground). Rch is always positive ($Rch > 0$). GPPch (Gross Primary Productivity) represents the photosynthetic CO_2 uptake by the groundnut plants and is negative during the day ($GPPch < 0$), and zero at night, when $FCO_2ch = Rch$.

Half-hourly FCO_2ch fluxes were partitioned as follows: (**1**) an Arrhenius-type function (Lloyd & Taylor, 1994) was fitted between nocturnal Rch and T_{soil} during nighttime periods, for each 5-days throughout the time series (Eq. 4). This empirical formulation is based on several key assumptions. First, the relationship between nocturnal respiration and soil temperature is assumed to follow an exponential response, reflecting the temperature sensitivity of respiration processes. Second, the model assumes temporal stability of the respiration–temperature relationship between night and day, allowing diurnal respiration to be extrapolated from fitted parameters in Eq.4 and daytime T_{soil}. Third, we assumed that no abrupt changes in substrate availability or soil moisture occur between day and night — conditions that could otherwise disrupt the temperature–respiration relationship. These assumptions are widely applied in CO_2 flux partitioning approaches (Reichstein et al., 2005; Lasslop et al., 2010). (**2**) Diurnal Rch was estimated by applying the Lloyd & Taylor function, previously calibrated on nocturnal data, to the corresponding daytime T_{soil} measurements for each 5-day interval. (**3**) GPPch was subsequently derived as the residual component of the net CO_2 flux during the day, according to:

$$\textbf{nocturnal Rch} = \mathbf{R_{ref}} \,.\, \textbf{exp}\,[\mathbf{E_0}\,\left(\frac{1}{\mathbf{T_{ref}-T_0}} - \frac{1}{\mathbf{T_{soil}-T_0}}\right)] \qquad \textbf{(Eq. 4)}$$

where R_{ref} (µmol CO_2 m^{-2} s^{-1}) is a fitted parameter representing the base respiration at the reference temperature [T_{ref} (K), (set at 288.15 K)]. E_0 (K) is the temperature sensitivity (set at 250 K), T_{soil} (K) the soil temperature (K), and T_0 (K) is kept constant at 231.13 K, according to Lloyd & Taylor (1994).

$$\textbf{GPPch} = \textbf{diurnal FCO}_2\textbf{ch} - \textbf{diurnal Rch} \qquad \textbf{(Eq. 5)}$$

where diurnal FCO_2ch and diurnal Rch represent the daytime net CO_2 fluxes and respiration in µmol CO_2 m^{-2} s^{-1}, respectively.

2.3.4. Gap-filling procedure

Missing Rch data were gap-filled using the model derived from Eq. 4 (Lloyd & Taylor, 1994). Prior to gap-filling GPPch, raw data were standardised by LAI to reduce variability between chambers due to differences in leaf surface area (Eq. 6). A light-response model was then fitted to the standardised GPPch data, every 5-day period, to gap-fill missing values. The model is based on a rectangular hyperbolic function that describes the relationship between photosynthetic CO_2 uptake and incoming global radiation (Rg) (Eq. 7). It corresponds to a Michaelis–Menten-type light-response curve, commonly used in ecosystem carbon exchange studies (Falge et al., 2001; Lasslop et al., 2010).

$$\textbf{GPPch.stand} = \frac{\textbf{GPPch}}{\textbf{LAIch}} * \textbf{LAI.field} \quad \textbf{(Eq. 6)}$$

where GPPch.stand (µmol CO_2 m^{-2} s^{-1}) is the standardised GPPch. LAIch and LAI.field (m^2 leaves m^{-2} soil) represent the groundnut LAI inside the chambers and the groundnut + weeds +cowpea LAI for the whole field, respectively.

$$\textbf{GPP} = \frac{\alpha\beta\textbf{Rg}}{\alpha\textbf{Rg}+\beta} \qquad \textbf{(Eq. 7)}$$

where α (µmol CO_2 J^{-1}) represents the light use efficiency of the groundnut plants inside the chambers, and refers to the initial slope of the light-response curve, β (µmol CO_2 m^{-2} s^{-1}) is the maximum CO_2 uptake rate by the groundnut plants at light saturation, and Rg the global radiation (W m^{-2}).

2.3.5. Comparing chamber-based (Ch) and Eddy Covariance (EC) methods

Chamber measurements were upscaled to field-level CO_2 fluxes and compared with EC-derived fluxes. Before comparison, a correction was applied (Eq. 6) to account for differences in LAI between chambers (LAIch) and the field (LAI.field), due to the presence of cowpea and weeds in the field but not in the weeded chambers.

Upscaling considered tree cover, with FS and Sh chamber fluxes weighted at 90% and 10%, respectively. Rch.stand and GPPch.stand, representing chamber-based respiration and

photosynthesis at field scale. These fluxes were compared, on a half-hourly basis, to EC-derived Reco.EC and GPP.EC (Table S4). The November–December transition period was excluded due to weed-driven uncertainties after groundnut harvest.

During the rainy season (*F. albida* leafless), GPP.EC represented ground vegetation (groundnut, cowpea, weeds), while Reco.EC included autotrophic respiration from all vegetation (including trees), and heterotrophic respiration (Reco.EC = Ra tree below-ground + Ra tree above-ground + Ra groundnut + Ra cowpea + Ra weeds + Rh). Rch.stand could not be fully upscaled to the field due to uncertainty in its partitioning between Ra and Rh. Rch.stand accounted only for Ra tree below-ground, Ra groundnut, and Rh.

In the dry season (leafy trees, bare soil), GPP.EC reflected tree photosynthesis only (GPP tree), while GPPch.stand was nil. Reco.EC included Ra tree (above- and below-ground) and Rh. Rch.stand, measured on bare soil, represented only Ra tree below-ground + Rh.

2.3.6. Contribution of trees to full ecosystem respiration and photosynthesis

During the dry season, when the trees (*F. albida*) maintained their foliage, a comparison between chamber and EC measurements allowed for the estimation of the contribution of the above-ground tree compartments to total ecosystem respiration (Table S4). Based on this estimate, total tree respiration (Ra tree) was then calculated under the assumption that the tree root systems (Ra tree below-ground) represent ⅓ of the above-ground biomass (Jackson et al. 1996).

Given the GPP measured during the dry season was equivalent to GPP of trees (GPP trees) from EC measurements, the carbon use efficiency of the trees (CUE tree) was then calculated (Table S4). The resulting CUE value was assessed to determine whether it approximated the typical value of 0.5, which is often used as a default in ecosystem models (Zhou et al., 2019; 2020).

2.3.7. Net annual vertical C balance at the ASPS scale

The net C balance of CO_2 fluxes in a yearly basis was estimated for chambers and EC measurements in Mg C-CO_2 ha^{-1}. The chambers CO_2 flux balances were obtained by calculating the annual sum of the net CO_2 flux measurements and then weighting with the tree cover rate (10% for the Sh, 90% for the FS). These annual balances for the field are considered apparent representing vertical CO_2 exchanges only, as they do not account for the biomass exported from the field after the harvest, the decomposition of which therefore escaped both the chambers and the EC. Additionally, the inputs and the outputs of faecal matter resulting from livestock wandering during the dry season were not quantified and are therefore neglected. The objective here is to compare two approaches at different scales using vertical net C balances, rather than to provide an absolute C budget which would also include horizontal transfers of carbon.

2.4. Statistical analyses

Statistical analyses were performed using the R software (R. Core Team, 2023). To compare the mean values of climatic parameters between the FS and Sh situations, a non-parametric Mann-Whitney test was used when both the normality (shapiro.test) and the homogeneity of the variance (Levene Test, R package 'Car'; Fox et al., 2023) were not confirmed. This approach was similarly applied to compare the seasonal dynamics of CO_2 fluxes between FS and Sh, as well as between the chamber-based and Eddy Covariance (EC) methods. Means and standard deviations were computed using the 'skim' function from the R package 'skimr' (Waring et al., 2022).

Respiration (Rch) (Eq. 4) and GPP (GPPch) models (Eq. 7) were fitted using non-linear least squares regression, implemented in the library in R 'nls.multstart' (Padfield et al., 2025). For the GPPch model, parameters α and β with non-significant p-values were removed, and then the remaining values were interpolated and smoothed using a 'spline' function from the 'zoo' library in R (Zeileis et al., 2024). Ordinary least-square linear regressions were fitted between the measured and the modeled values derived from. Model performance of Eq. 4 and Eq. 7 was evaluated by fitting ordinary least-square linear regressions between the measured and the modeled values using R^2, root mean square error (RMSE), and the bias metrics. Given that the primary objective of these equations was to accurately reproduce the seasonal dynamics of the CO_2 fluxes to fill gaps in data, particular emphasis was placed on R^2, with a higher value reflecting a better fit of the model to the measurements.

Correlation analysis was conducted between chamber CO_2 fluxes (FCO_2ch, Rch, GPPch) and soil temperature (T_{soil}, °C), air temperature (T_{air}, °C), VWC, the leaf area index of groundnut plants in the chambers (LAIch), and the fitted parameters for respiration — R_{ref} — and photosynthesis — α and β. This analysis was performed using the 'cor.test' function from the 'stats' package in R (Lüdecke et al., 2021), applying the Spearman method.

The threshold of the daily mean soil temperature (T_{soil}, °C) at which the cumulative daily respiration (Rch, g C-CO_2 m^{-2} d^{-1}) began to decline was determined using segmented regression from the R package 'segmented' (Muggeo, 2003). The associated uncertainty (standard error) of this estimate was evaluated through a bootstrap procedure.

The standard error of the total annual flux was estimated using the error propagation method. This calculation considered the mean standard deviation of daily fluxes (g C–CO_2 d^{-1}) and the effective number of measurement days (365). For each FS and Sh condition, the mean daily standard deviation was multiplied by the square root of 365 to obtain the annual standard error. The resulting values were then weighted by 90% for FS and 10% for Sh to derive the overall standard error of the annual flux sum, which was subsequently converted to Mg C–CO_2 ha^{-1}.

3. Results

3.1. Microclimatic conditions

During the experiment, the cumulative rainfall was 550 mm, which was representative of the interannual average. Precipitations were lowest in July and highest between August and September, a period that typically corresponds to the peak of the rainy season (Fig. 2a). Global radiation ranged between 5.8 and 32.4 MJ m^{-2} d^{-1} (data not shown). The daily mean VWC in the chambers showed significant variation, ranging from 1% at the end of the dry season to a maximum of 30% during the rainy season (Fig. 2a). While VWC was similar during the rainy season, it remained consistently higher in FS than in Sh throughout the dry season ($p < 0.05$), which was unexpected. However, it should be noted that the last rain of October 2021 recharged the FS chambers more effectively, likely due to foliage rainfall interception by *F. albida* which had just put on leaves at that time, potentially explaining this discrepancy in VWC.

Within the chamber, the daily mean T_{soil} ranged from 26°C in April to 37.5°C at the end of the dry season (Fig. 2b), while T_{air} varied between 23.7°C and 35.5°C (Fig. 2c). However, during instantaneous daily peaks, T_{soil} could exceed 45°C in May (data not shown). As expected, both daily mean T_{soil} and T_{air} were significantly higher in FS compared to Sh situations ($p < 0.05$), with T_{soil} and T_{air} averaging respectively 1°C and 0.5°C lower under the tree canopy.

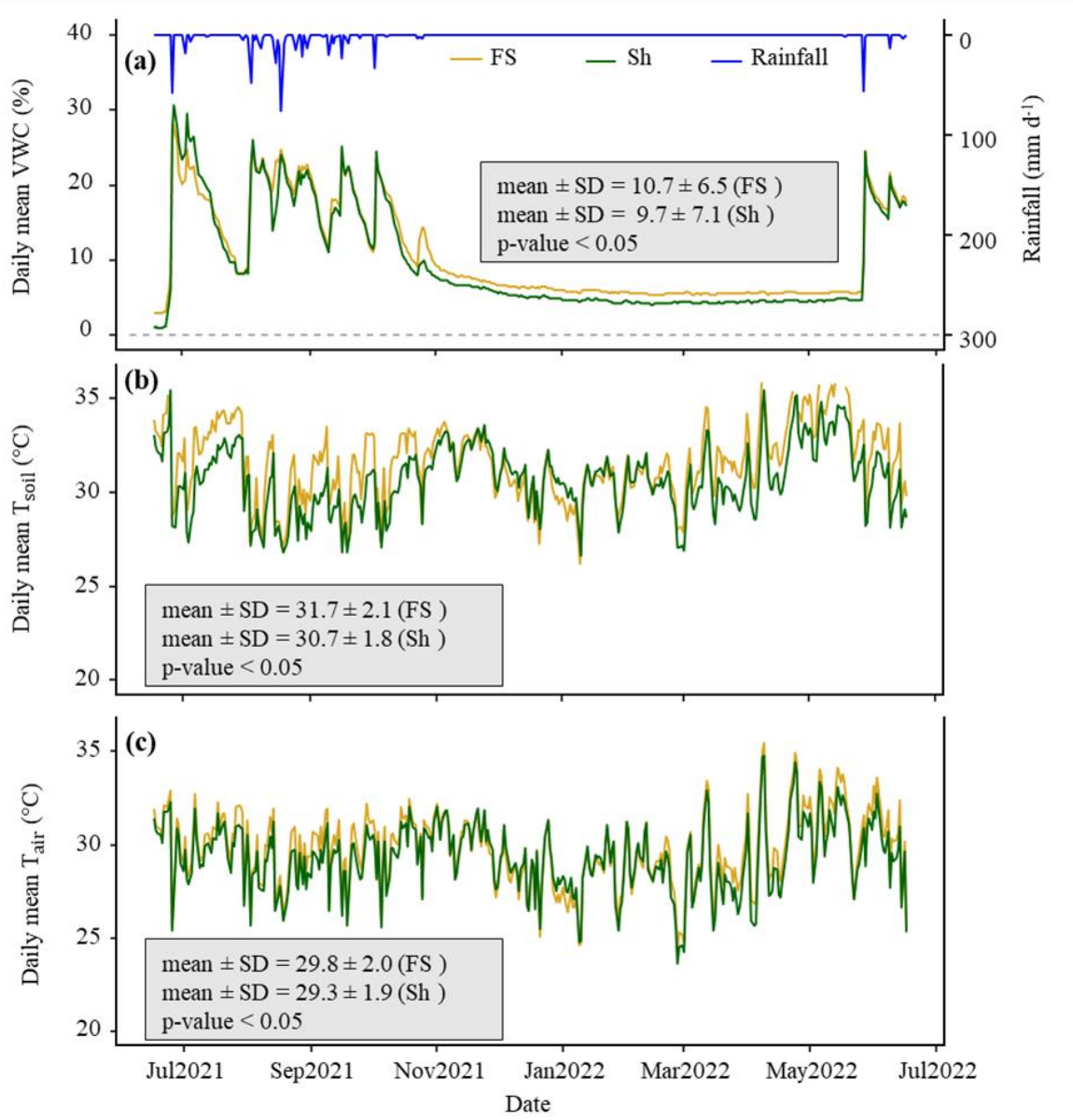

353 Fig. 2: One-year time series of daily average microclimatic parameters measured inside the
354 chambers.

355 (a) volumetric soil water content (VWC) at a depth of 6 cm (%). (b) soil temperature (T_{soil}) at a depth of 6
356 cm (°C), (C) air temperature (T_{air}) at a height of 15 cm (°C). The blue line depicts the daily rainfall (mm d^{-1})
357 throughout the year. FS: Full sun chambers; Sh: Shaded chambers. Mean and SD represent respectively the
358 mean value and the standard deviation. The p-value indicates the probability associated with the statistical
359 test, assessing the differences in means between FS and Sh with the significance level α set to 0.05.

3.2. Modeling the chamber-based total respiration (Rch) and photosynthesis (GPPch)

3.2.1. Dynamics of reference respiration, light use efficiency, and maximum CO_2 uptake rate at light saturation (R_{ref}, α., and β)

The reference respiration (R_{ref}) showed comparable seasonal dynamics both at a distance from the trees (FS) and under the tree canopies (Sh) (Fig. S4). In both situations, R_{ref} showed strong variability during the rainy season, peaking in September 2021 at 2.4 µmol CO_2 m^{-2} s^{-1} for FS and 2.9 µmol CO_2 m^{-2} s^{-1} for Sh (Table S3). In contrast, during the dry season — from November 3, 2021 (after harvest) until the onset of the following rainy season (June 2022) — R_{ref} values dropped both for FS and Sh, averaging 0.3 ± 0.5 µmol CO_2 m^{-2} s^{-1} for FS and 0.5 ± 0.6 µmol CO_2 m^{-2} s^{-1} for Sh. This represents a reduction by a factor of 8 for FS and 6 for Sh compared to the rainy season. The mean annual R_{ref} values were significantly higher under Sh than in FS, with value approximately 1.5 times greater (Table S3).

Regarding GPP in chambers, the light use efficiency (α) and the maximum CO_2 uptake by groundnut plants in the chambers (β), also reached their maximum during the peak of the rainy season (Fig. S5, a and b). The maximum value of α reached 0.2 µmol CO_2 J^{-1} in FS and 0.3 µmol CO_2 J^{-1} in Sh (Table S3). Similarly, the maximum values of optimum CO_2 uptake rate at light saturation (β) were 40.2 µmol CO_2 m^{-2} s^{-1} for FS and 42.8 µmol CO_2 m^{-2} s^{-1} for Sh (Table S3). In the dry season, when photosynthetic activity ceased in the chambers, both α and β were assumed to be nil (Fig. S5, a and b). On average, α and β were significantly higher in Sh than in FS, by a factor of 1.7 and 1.2, respectively (Table S3). We noted that the decline in photosynthetic activity of the groundnut crop occurred earlier and rapidly at a distance from the trees (FS), as reflected by the sharply observed recession of α and β in FS.

3.2.2. Dynamics of nocturnal respiration in chambers

The averaged nocturnal respiration (nocturnal Rch) calculated from the measurements across each treatment (FS and Sh), showed similar seasonal patterns (Fig. 3, a and c). Following the first rains, Rch values increased dramatically, with a nocturnal 'Birch effect' — a sudden pulse of CO_2 release following soil rewetting — observed to be more pronounced under Sh compared to FS, approximately by a factor of 2. At the peak of the rainy season (September), the maximum nocturnal Rch values reached approximately 6.0 µmol CO_2 m^{-2} s^{-1} in FS and 9.0 µmol CO_2 m^{-2} s^{-1} in Sh (Fig. 3, a and c). Thereafter, nocturnal Rch declined well before the groundnut harvest along with the rainfall spacing and the groundnut crop senescence (data not shown). During the dry season nocturnal Rch continued to decrease, with maximum values around 1.0 µmol CO_2 m^{-2} s^{-1} in FS and 2.0 µmol CO_2 m^{-2} s^{-1} in Sh (Fig. 3, a and c).

393 The modeled nocturnal Rch values closely matched the measured nocturnal Rch values (mean
394 across four chambers per treatment), as indicated by the model performance metrics ($R^2 = 0.9$,
395 with bias and RMSE values of 0.3 and 0.5 μmol CO_2 m^{-2} s^{-1}, respectively, for FS; $R^2 = 0.7$, with bias
396 and RMSE values of 0.4 and 0.6 μmol CO_2 m^{-2} s^{-1}, respectively, for Sh) (Fig. 3, b and d). Similarly,
397 the daily mean modeled values also fitted well with the measured values, with FS showing (mean
398 $\pm$ standard deviation) 0.9 $\pm$ 0.9 μmol CO_2 m^{-2} s^{-1} (modeled) and 1.2 $\pm$ 1.2 μmol CO_2 m^{-2} s^{-1}
399 (measured), while Sh recorded 1.4 $\pm$ 0.9 μmol CO_2 m^{-2} s^{-1} (modeled) and 1.5 $\pm$ 1.2 μmol CO_2 m^{-2}
400 s^{-1} (measured). Given the close match between the measured and modeled values, the fitted
401 model parameters were used subsequently to fill data gaps and estimate diurnal Rch values, as
402 presented in Fig. 4, a and c.

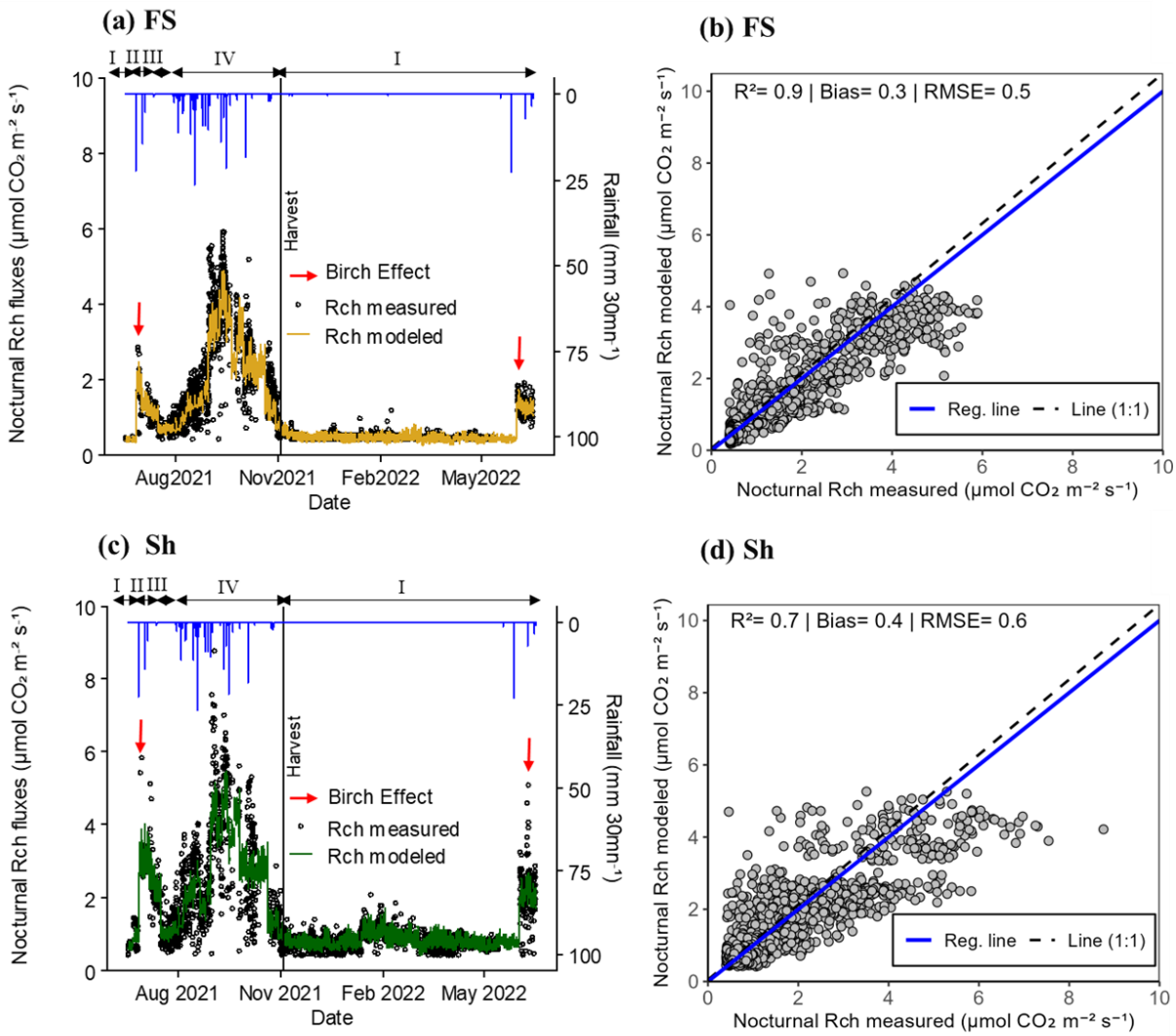

Fig. 3: Dynamics of instantaneous nocturnal CO_2 fluxes in chambers in Full sun (FS; a and b) and Shaded (Sh; c and d) environments (data filtered based on R^2 of the CO_2 variation over the time of chamber closure and Minimum Detectable Flux, Eq.2).

(a) and (c): measured nocturnal respiration in chambers (Rch: black dots; average of measurements in 4 chambers per location) vs. modeled (coloured line). The vertical black line indicates the harvest date of groundnuts inside the chambers. The red arrows indicate the 'Birch' effect and the blue line represents the rainfall (mm $30mn^{-1}$). Roman numerals (above the black arrows) refer to vegetation conditions prevailing inside the chambers, i.e. (I) bare soil, (II) weeds, (III) weeds + groundnuts, and (IV) groundnuts only.
(b) and (d): scatter plot between measured and modeled nocturnal Rch. The solid blue line indicates the regression line and the dashed black one the (1:1) line RMSE and bias are expressed as fluxes (in µmol CO_2 m^{-2} s^{-1}). Each point represents the mean value from 4 chambers within the FS or Sh environments.

3.2.3. Dynamics of daytime fluxes in chambers

The measured GPPch.stand, as well as GPP modeled with Eq. 6, showed similar seasonal dynamics inFS and Sh (Fig. 4, a and c). The fluxes peaked during the rainy season (Fig. 4a and c), coinciding with periods of vigorous vegetative growth characterised by a high leaf area index (LAIch) of groundnut plants within the chambers (Fig. S3). The maximum calculated and standardised GPPch values reached -50 µmol CO_2 m^{-2} s^{-1} for FS and -37 µmol CO_2 m^{-2} s^{-1} for Sh. As expected, these fluxes were nil during the dry season when the soil was bare (Fig. 4, a and c).

The modeled GPPch values closely followed the same trends as the calculated values, although model performance was slightly better for FS ($R^2 = 0.7$ with bias and RMSE values of 4.2 and 6.1 µmol CO_2 m^{-2} s^{-1}, respectively) compared to Sh ($R^2 = 0.6$ with bias and RMSE values of 6.1 and 5.6 µmol CO_2 m^{-2} s^{-1}, respectively) (Fig. 4, b and d).

The calculated diurnal respiration values (diurnal Rch calculated) for FS and Sh revealed a 'Birch effect' similar to that observed during the night, though slightly more pronounced under Sh by a factor of 1.2. Diurnal Rch values increased significantly during the rainy season, reaching a maximum of 6.0 µmol CO_2 m^{-2} s^{-1} for both FS and Sh (Fig. 4, a and c). In the dry season, on bare soil, these values declined, with maximum respiration reaching only 0.5 µmol CO_2 m^{-2} s^{-1} for both situations (FS and Sh) (Fig. 4, a and c).

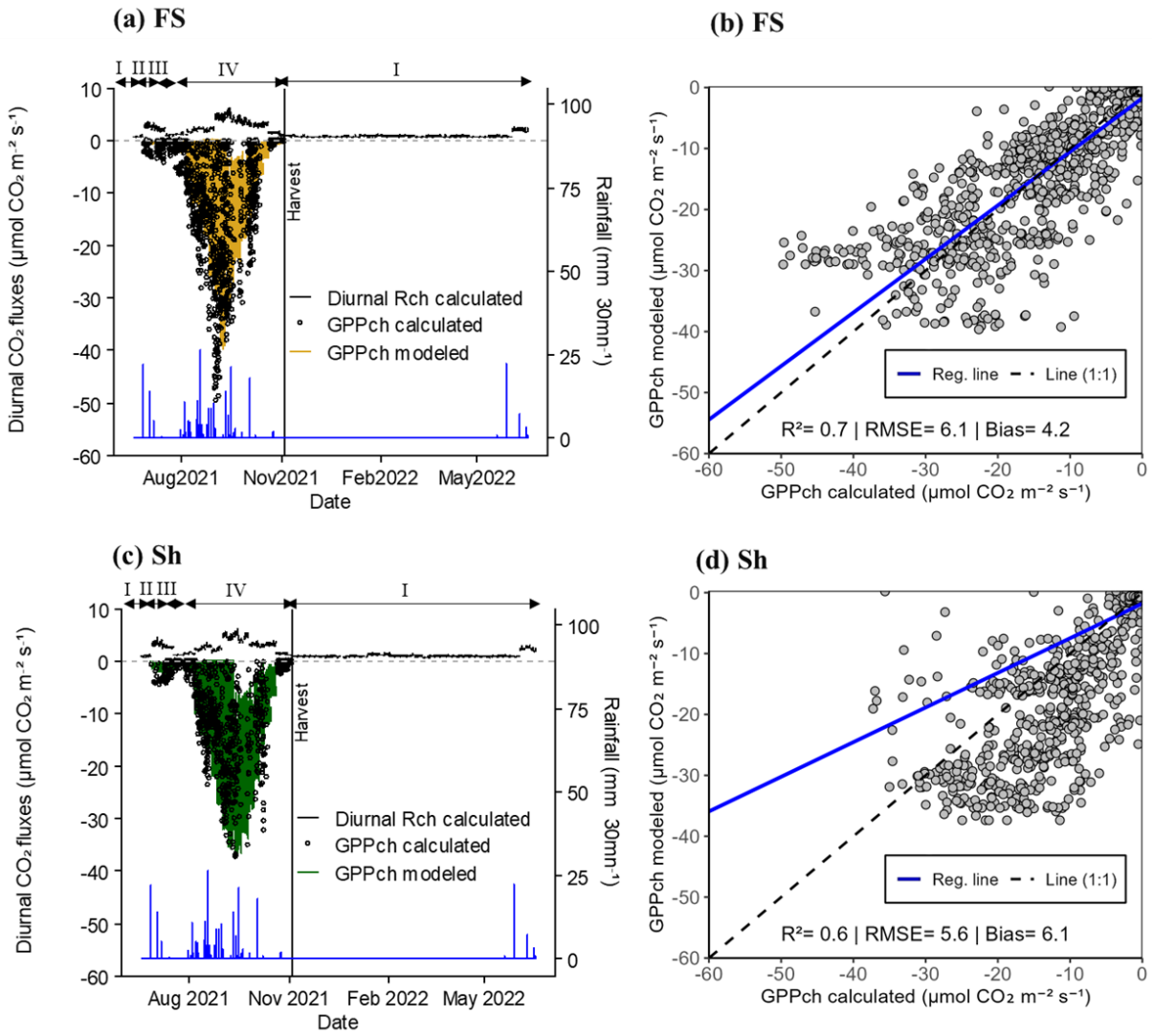

431 Fig. 4: Dynamics of instantaneous diurnal CO_2 fluxes in chambers in Full sun (FS; a and b) and
432 Shaded (Sh; b and d) environments (filtered based on R^2 of the CO_2 variation over the time closure
433 in FS and Sh and Minimum Detectable Flux, Eq.2).

434 (a) and (c): non-gap-filled diurnal Rch calculated (black line, positive values; average of measurements in
435 4 chambers per location) and GPPch calculated from Eq.5 then standardised for LAI (black dots, negative
436 values) and modeled (coloured line, negative values). The vertical black line indicates the harvest date of
437 groundnuts inside the chambers and the blue line represents the rainfall (mm $30mn^{-1}$). Roman numerals
438 (above the black arrows) refer to conditions prevailing inside the chambers, i.e., (I) bare soil, (II) weeds,
439 (III) weeds + groundnuts, and (IV) groundnuts.
440 (b) and (d): scatter plot between calculated and modeled GPPch. The solid blue line indicates the regression
441 line and the dashed black one the (1:1) line. RMSE and bias are expressed as fluxes (in µmol CO_2 m^{-2} s^{-1}).
442 Each point represents the mean value from 4 chambers within the FS or Sh environments.

3.3. Dynamics of daily cumulative CO_2 fluxes in chambers

The seasonality of daily cumulative of GPPch.stand showed similar dynamics between FS and Sh, with higher variability during the rainy season than during the dry season (Fig. 5). Daily total Rch peaked during the rainy season at 5.1 g C-CO_2 m^{-2} d^{-1} for FS and 5.4 g C-CO_2 m^{-2} d^{-1} for Sh, while the maximum GPPch.stand values were comparable at around -15.0 g C-CO_2 m^{-2} d^{-1} for both FS and Sh (Table 1; Fig. S7, a, b, c, and d). In the dry season, Rch decreased (Fig. 5), averaging 0.5 g C-CO_2 m^{-2} d^{-1} for FS and 1.0 g C-CO_2 m^{-2} d^{-1} for Sh. GPPch declined well before harvest (senescence) and remained nil during the dry season (Fig. 5). During the rainy season FCO_2ch peaked in absolute value at around 11.0 g C-CO_2 m^{-2} d^{-1} for FS and Sh (Fig. 5) (Table 1; Fig. S7, e and f), while FCO_2ch values were the same as Rch during the dry season. In absolute terms, the mean Rch and GPPch were significantly higher under Sh as compared to FS, by factors of 1.3 and 1.2, respectively. Conversely, the mean FCO_2ch was significantly higher in absolute value under FS (0.4 g C-CO_2 m^{-2} d^{-1}) than under Sh (0.2 g C-CO_2 m^{-2} d^{-1}) (Table 1).

The annual cumulative Rch values were 392.8 g C-CO_2 m^{-2} for FS and 574.5 g C-CO_2 m^{-2} for Sh. The GPPch fluxes reached -539.5 g C-CO_2 m^{-2} for FS and -632.6 g C-CO_2 m^{-2} for Sh. The net annual cumulative C exchange (FCO_2ch) was -146.7 g C-CO_2 m^{-2} in FS and -58.1 g C-CO_2 m^{-2} in Sh.

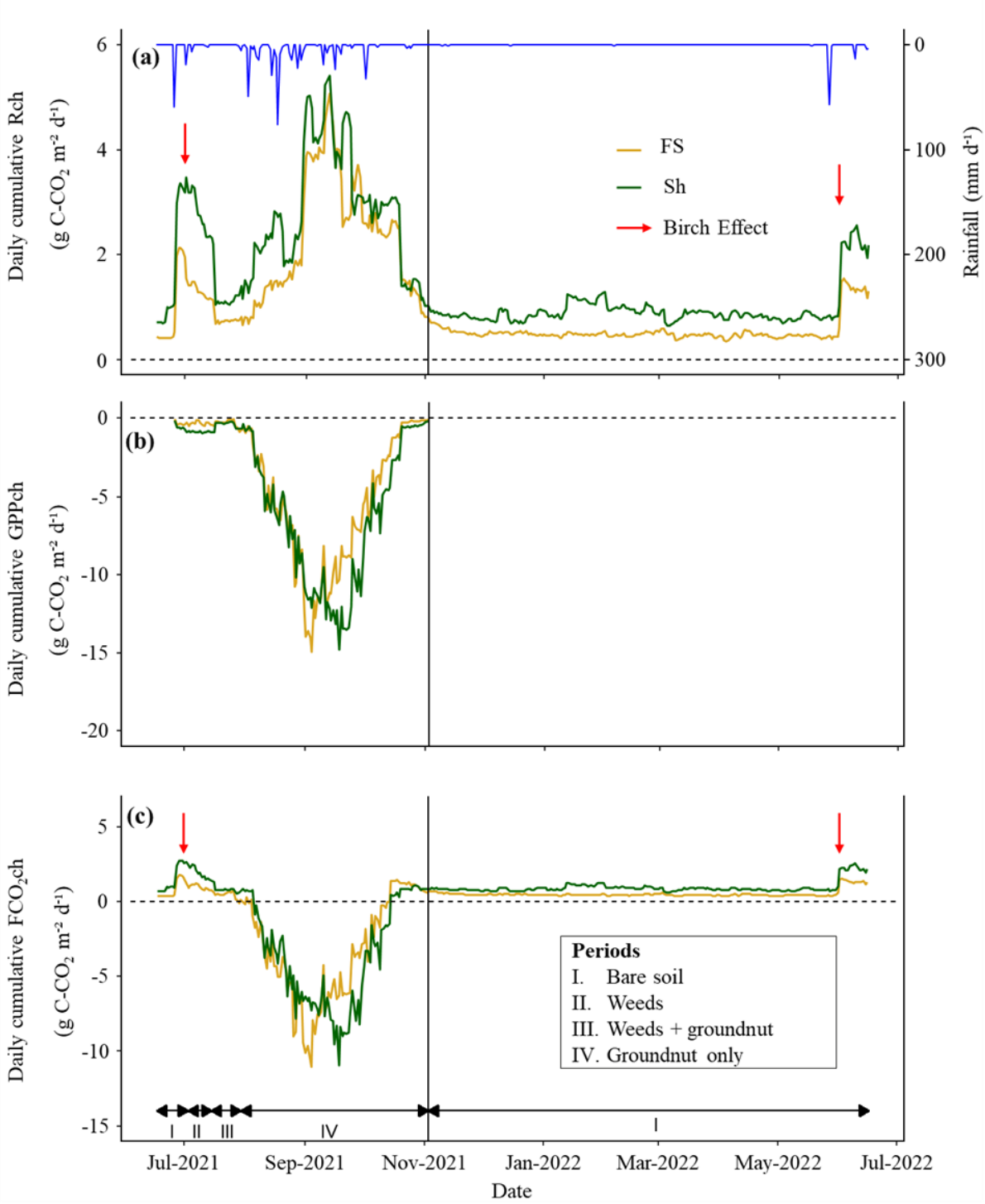

459 Fig. 5: Seasonal dynamics of daily gap-filled cumulative fluxes (in gC-CO_2 m^{-2} d^{-1}) in chambers.

460 (a) soil+crop respiration (Rch), (b) photosynthesis (GPPch, standardised for LAI) and (c) net CO_2 exchange
461 (FCO_2ch). The yellow and green solid lines compare the FS and Sh environments, respectively. The vertical
462 black line indicates the harvest date of groundnuts inside the chambers. The blue line depicts the daily
463 cumulative rainfall (mm d^{-1}) throughout the rainy season, and the red arrow indicates the 'Birch'
464 effect. Roman numerals (above the black arrows) in (a) and (c) refer to the prevailing conditions inside the
465 chambers: (I) bare soil, (II) weeds, (III) weeds + groundnuts, (IV) groundnuts.

Table 1: Comparison of daily cumulative and gap-filled chamber CO_2 fluxes (Rch, GPPch standardised for LAI, and FCO_2ch in g C-CO_2 m^{-2}) in the FS and Sh condition.

	Annual sum	Daily Mean ±SD	Min	Max	Mann-Whitney test
(g C-CO_2 m^{-2})	.yr^{-1}	.d^{-1}	.d^{-1}	.d^{-1}	
Rch					
FS	392.8	1.1 ± 0.9	0.4	5.1	*
Sh	574.5	1.6 ± 1.1	0.6	5.4	
GPPch					
FS	-539.5	-4.1 ± 4.3	< -0.1	-14.9	*
Sh	-632.6	-4.8 ± 4.6	< -0.1	-14.8	
FCO_2ch					
FS	-146.7	-0.4 ± 2.4	-11.0	1.8	*
Sh	-58.1	-0.2 ± 2.7	-10.9	2.8	

Annual sum corresponds to the annual cumulative fluxes (g C-CO_2 m^{-2} yr^{-1}). Mean, SD, Min, and Max represent respectively the mean, standard deviation, minimum, and maximum values at the daily scale (g C-CO_2 m^{-2} d^{-1}). Asterisks (*) indicate the p-values from the Mann-Whitney test, used to assess differences in mean between FS and Sh ($p < 0.05$). Positive values indicate CO_2 emissions, while negative values represent CO_2 uptake.

3.4. Drivers of daily respiration and photosynthesis in chambers

The chamber-based daily cumulative respiration (Rch) and GPPch showed significant and positive correlations with the leaf area index (LAIch), both at a distance from the trees (FS) and under the trees (Sh) (Table 2). The influence of LAIch on GPPch was stronger ($r = 0.86$ for FS and Sh) than its influence on Rch ($r = 0.60$ for FS; $r = 0.69$ for Sh). Soil VWC was also positively correlated with Rch and GPPch, both in FS and Sh. However, the influence of soil VWC on Rch was stronger under Sh compared to FS, while its influence on GPPch was similar in both situations (FS and Sh). Soil temperature showed weak negative correlations with Rch (in FS and Sh) and with GPPch (only in Sh). Finally, no significant correlations were found between T_{air}, and any of the CO_2 fluxes (Table 2).

Table 2: Spearman correlation matrix based on daily cumulative and gap-filled CO_2 fluxes from full year chamber measurements (g C-CO_2 m^{-2} d^{-1}) with microclimatic parameters.

Parameters	Condition	r-coef. (Rch)	p (Rch)	r-coef. (GPPch)	p (GPPch)
T_{soil}	FS	-0.25 ***	7.47×10^{-4}	ns	1.18×10^{-3}
	Sh	-0.28 ***	9.69×10^{-14}	-0.38 ***	2.88×10^{-7}
T_{air}	FS	ns	0.22	ns	0.35
	Sh	ns	0.98	ns	0.15
VWC	FS	0.51 ***	3.00×10^{-34}	0.75 **	6.73×10^{-3}
	Sh	0.78 ***	1.29×10^{-66}	0.75*	0.02
LAIch	FS	0.60 ***	1.11×10^{-61}	0.86 ***	2.23×10^{-8}
	Sh	0.69 ***	6.08×10^{-69}	0.86 ***	2.11×10^{-12}

Spearman correlation coefficients (r-coef.) between daily cumulative and gap-filled CO_2 flux components (Rch and GPPch, with GPPch in absolute terms) and daily mean microclimatic parameters in full sun (FS) and shaded chambers (Sh). T_{soil} (°C) is the daily mean soil temperature at 6 cm depth, T_{air} (°C) the daily mean air temperature at 15 cm height, VWC (%) the daily mean volumetric water content (VWC, %), and LAIch (m^{-2} leaf m^{-2} soil) the chamber leaf area index value for a given day. Letter p represents the p-value and significance levels are indicated by (*** $p<0.001$; ** $p<0.01$; * $p<0.05$); ns $p > 0.05$.

3.5. Comparison of respiration and GPP measurements between chambers (Ch) and Eddy Covariance (EC) methods

The chamber-based daily total CO_2 fluxes, gap-filled and weighted according tree cover were compared with the fluxes obtained using the EC method (Fig. 6).

During the rainy season, both total respiration and GPP showed comparable dynamics between the two methods, with synchronised peaks and higher variability compared to the dry season (Fig. 6). The maximum value of Reco.EC, peaked at 13.5 g C-CO_2 m^{-2} d^{-1} (Table 3). The initial value of Rch.stand was comparable to Reco.EC but peaked only at 5.1 g C-CO_2 m^{-2} d^{-1} (Table 3), meaning a third of the peak of Reco.EC. The maximum GPP, was -14.3 g C-CO_2 m^{-2} d^{-1} and -14.6 g C-CO_2 m^{-2} d^{-1} for GPP.EC and GPPch.stand, respectively (Table 3). This indicates that the LAI-based standardisation and upscaling approach were realistic, at least up to the peak of groundnut growth.

On average, Reco.EC was significantly higher than Rch.stand, by a factor of 2.3. GPP.EC was also significantly higher than GPPch.stand, but only by a factor of 1.2 (Table 3).

During the dry season, Reco.EC and Rch.stand gradually decreased. The values for Reco.EC remained higher than for Rch.stand, which was fairly consistent with the contribution of the Ra tree above-ground compartment, even if this difference seemed to disappear at the end of the dry season (Fig. 6). The measured 'Birch effect' was highest for Rch.stand in 2021, but was the opposite in 2022 due to a system failure at the beginning of the rainy season. The maximum value of GPP.EC reached -2.4 g C-CO_2 m^{-2} d^{-1} when the trees were at their maximum of foliage, after harvest and while weeds were still present in the field. However, after the harvest, chamber photosynthesis (GPPch.stand) was nil (Table 3).

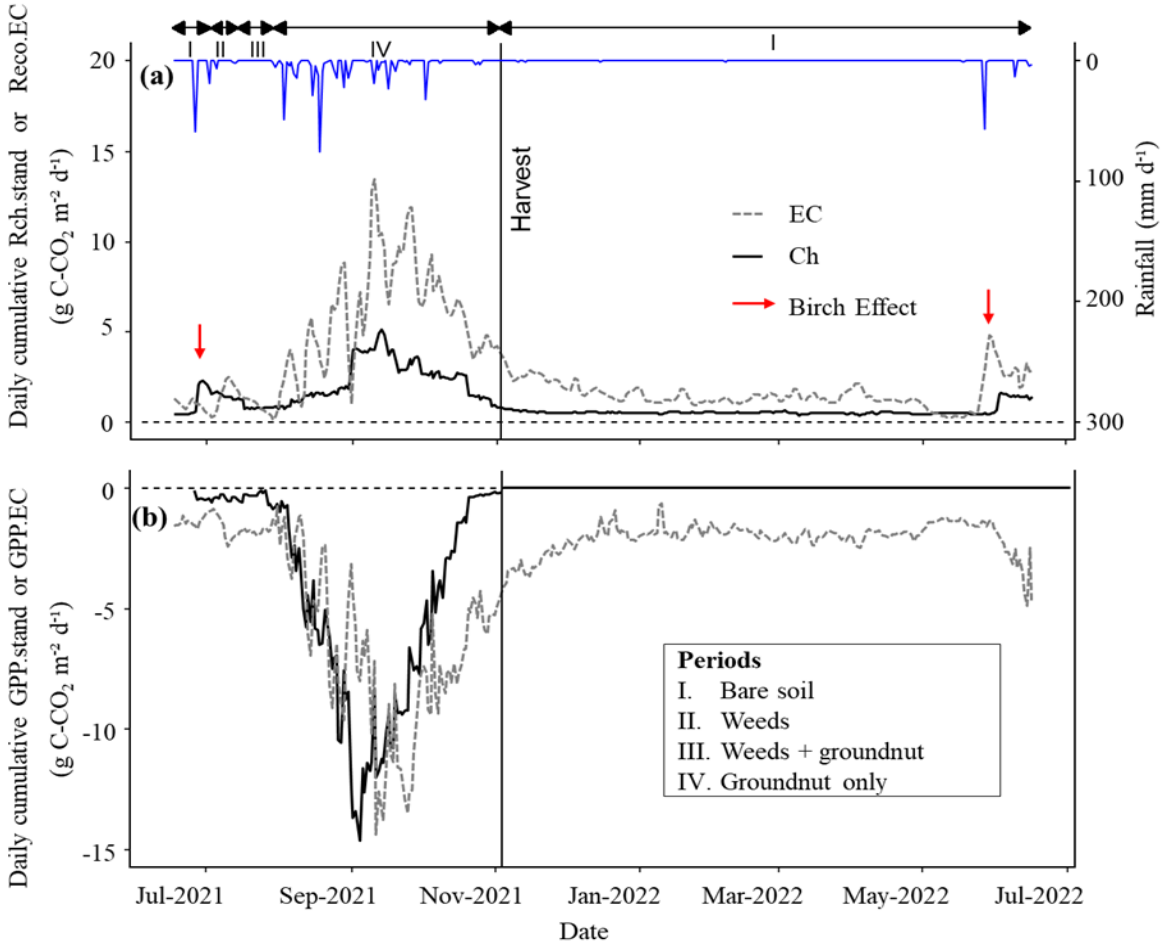

514 Fig 6: Comparing the seasonal dynamics of CO_2 fluxes between Eddy Covariance (EC)
515 measurements and upscaled chamber measurements (ch.stand).

516 (a) represent the seasonal dynamics of soil + crop respiration (Rch.stand) and ecosystem respiration
517 (Reco.EC) and (b) photosynthesis (GPP.stand and GPP.EC). The black and dashed grey lines show Ch and
518 EC seasonal dynamics, respectively. The vertical black line indicates the harvest date of groundnuts inside
519 the chambers. The blue line depicts the daily cumulative rainfall (mm d^{-1}), and the red arrow indicates the
520 'Birch' effect. Roman numerals (above the black arrows) refer to conditions prevailing inside the
521 chambers: (I) bare soil, (II) weeds, (III) weeds + groundnuts, (IV) groundnuts.

Table 3: Comparison of gap-filled CO_2 fluxes between Eddy Covariance (EC) and upscaled chamber (Ch.stand) measurements, by season (rainy or dry).

	Rainy season				Dry season			
	Daily Mean ± SD	Min	Max	Mann-Whitney test	Daily Mean ± SD	Min	Max	Mann-Whitney test
(g C-CO_2 m^{-2})	$.d^{-1}$	$.d^{-1}$	$.d^{-1}$		$.d^{-1}$	$.d^{-1}$	$.d^{-1}$	
Reco.EC or Rch.stand								
EC	4.6 ± 3.2	0.2	13.5	*	1.2 ± 0.4	0.3	2.1	*
Ch.stand	2.0 ± 1.1	0.5	5.1		0.5 ± 0.04	0.4	0.6	
GPP.EC or GPPch.stand								
EC	-5.1 ± 3.6	-0.7	-14.3	*	-1.7 ± 0.3	-0.6	-2.4	-
Ch.stand	-4.2 ± 4.3	<-0.1	-14.6		0	0	0	

Mean, SD, Min, and Max represent the daily mean fluxes, standard deviation, minimum, and maximum values, respectively (g C- CO_2 m^{-2} d^{-1}). The Asterisks (*) indicate the p-values from the Mann-Whitney test, used to assess differences in mean between EC and Ch. Positive values indicate CO_2 emissions, while negative values represent CO_2 uptake.

3.6. The contribution of F. albida to Reco and GPP

During the dry season, the cumulative contribution of *F. albida* to ecosystem respiration (Ra tree) was 139.6 g C-CO_2 m^{-2}. This represent 14% of the total annual cumulative Reco, which was estimated at 1000.0 g C-CO_2 m^{-2} (Table S4). The contribution of trees (GPP tree) to total annual GPP in absolute term was 270.2 g C-CO_2 m^{-2}, equivalent to ~23% of the total annual cumulative GPP of the ecosystem measured by EC (1180.0 g C-CO_2 m^{-2}) (Table S4).

The ratio between these two components (Ra tree / GPP tree) in absolute terms was 0.52, reflecting a carbon use efficiency (CUE) of 0.48 (Table S4).

3.7. Annual vertical CO_2 balances at the field-scale

The upscaled chamber-based annual cumulative total respiration flux (Rch.stand) was estimated to be 4.1 $\pm$ 0.18 Mg C-CO_2 ha^{-1} (Table 4). In comparison, the annual Reco.EC was 10.0 $\pm$ 0.49 Mg C-CO_2 ha^{-1} (Table 4), more than two times larger than Rch.stand.

The upscaled GPPch.stand reached an annual cumulative value of -5.5 $\pm$ 0.83 Mg C-CO_2 ha^{-1}, whereas the annual cumulative GPP.EC was -11.8 $\pm$ 0.53 Mg C-CO_2 ha^{-1} (Table 4).

The net annual vertical C balance, based on both methods, was estimated at -1.4 $\pm$ 0.46 Mg C-CO_2 ha^{-1} for chambers (FCO_2ch.stand) and -1.8 $\pm$ 0.17 Mg C-CO_2 ha^{-1} for Eddy Covariance (NEE.EC) (Table 4).

543 Table 4: Annual budget of CO_2 fluxes based on Eddy Covariance (EC) and upscaled chamber
544 methods (Ch.stand).

	Annual sum (Mg C-CO_2 ha^{-1})	Std error (Mg C-CO_2 ha^{-1})
Reco.EC or Rch.stand		
EC	10.0	0.49
Ch.stand	4.1	0.18
GPP.EC or GPPch.stand		
EC	-11.8	0.53
Ch.stand	-5.5	0.83
NEE.EC or FCO_2ch.stand		
EC	-1.8	0.17
Ch.stand	-1.4	0.46

545 Annual sum corresponds to the annual cumulative fluxes for full year measurements (Mg C-CO_2 ha^{-1}). EC
546 refers to fluxes measured by the Eddy Covariance method, and Ch refers to the fluxes measured by
547 chambers, which are then upscaled to the whole field. Rch.stand represents the chamber respiration, while
548 Reco.EC denotes the ecosystem respiration according to the EC method. GPP.EC and GPPch.stand are the
549 gross primary production or photosynthesis flux, measured by EC and Ch methods, respectively. NEE.EC
550 and FCO_2ch.stand represent the net ecosystem exchange for EC and Ch, respectively. The associated
551 standard error is denoted as Std error (Mg C-CO_2 ha^{-1}). Positive values indicate CO_2 emissions, while
552 negative values represent CO_2 uptake.

4. Discussion

4.1. Soil respiration modeling and limitations

In this study the Lloyd and Taylor (1994) model, based on a modified Arrhenius-type formulation, was used to model nocturnal soil respiration fluxes for estimating daytime respiration. Unlike the classical Arrhenius equation, this model includes the (Tsoil – T0) term in the denominator of the exponential expression (Eq. 4), which inherently limits the effects of high temperatures by progressively reducing the temperature sensitivity of soil respiration as temperatures rise above a given threshold. This structural feature produces a flattening of the respiration–temperature relationship at elevated temperatures, thereby preventing the overestimations (Lloyd and Taylor, 1994).

The Lloyd and Taylor model has successfully been widely applied, primarily in boreal and temperate ecosystems (Lasslop et al., 2010; Reichstein et al., 2003), and relies on the assumption of comparable thermal conditions between daytime and nighttime periods (Juszczak et al., 2012). In our study, instantaneous soil temperatures ranged from 20.7 to 45.8 °C during the day and from 22.1 to 45.0 °C at night, indicating largely overlapping thermal ranges between the two periods. Model parameters were recalibrated using five-day fixed windows, which provided sufficient temporal resolution while capturing seasonal dynamics of soil respiration.

This study represents one of the first applications of the Lloyd and Taylor model in a Sahelian semi-arid context. While Arrhenius based models are known to potentially overestimate fluxes under extreme temperatures due to physiological limitations, over the range of temperatures observed in this study, the modeled soil respiration was not overestimated (Fig. S6, a and b). Thus, the model used in this study appears to provide a realistic representation of soil respiration under local conditions. However, this conclusion is site-specific and should not be interpreted as a general validation of temperature-based models across all semi-arid environments. Such models should be systematically validated with respect to temperature to ensure their reliability.

4.2. Seasonality and drivers of chamber-based CO_2 fluxes

In our agroforestry context, seasonal variability in CO_2 fluxes closely followed rainfall dynamics, peaking during the wet season and declining sharply in the dry season, consistent with soil moisture depletion and crop senescence. This pattern is typical of semi-arid ecosystems (Ago et al., 2016a; Brümmer et al., 2008; Guillen-Cruz et al., 2023; Macharia et al., 2020; Mosongo et al., 2022; Wieckowski et al., 2024).

Respiration and photosynthesis were primarily driven by soil moisture and LAI, reflecting the system's sensitivity to water availability and crop dynamics. Soil moisture enhanced both processes by stimulating microbial activity and supporting plant growth (Borken et al., 2002;

Conant et al., 2004; Merbold et al., 2009; Yu et al., 2020; Zhao et al., 2016). The stronger correlation between soil moisture and respiration under *F. albida* canopy (Sh: $r = 0.78$) compared to full sun (FS: $r = 0.51$) suggests greater microbial sensitivity to moisture beneath trees. This likely reflects enhanced substrate availability, resulting in stronger post-rainfall respiration pulses (Meisner et al., 2015) and supporting the 'fertile island' effect, where trees improve local soil conditions (Eldridge et al., 2024). Photosynthetic capacity also responded to soil moisture, as shown by positive correlations with LAI and key physiological traits such as light use efficiency (α) and maximum CO_2 uptake rate (β) (Gonsamo et al., 2019; Qiu et al., 2023; Zhang et al., 2024).

In contrast, the influence of soil temperature (T_{soil}) on respiration was weakly negative in both FS and Sh, indicating a thermal threshold beyond which respiration declined —estimated at 32 ± 1.5 °C in FS and 29.5 ± 1.9 °C in Sh (Fig. S9, a and b), similar to findings in Eastern Ghana (Owusu et al., 2024). This inhibition likely results from decreased enzymatic and microbial activity under combined heat and water stress (Liu et al., 2018; Richardson et al., 2012). In semi-arid regions, soil respiration often becomes decoupled from temperature due to seasonal moisture constraints (Jia et al., 2020; Tucker & Reed, 2016; Warren, 2014), with microbial activity limited during dry periods despite favourable temperatures. This decoupling helps explain the weak or absent correlation between T_{soil} and soil moisture (Fig. S8, b), particularly under Sh ($r = -0.28$). Management practices such as organic inputs can also modulate these dynamics, adding further variability to soil respiration responses (Meena et al., 2020; Oyonarte et al., 2012; Rong et al., 2015; Xue & Tang, 2018).

4.3. Magnitude of chamber-based total CO_2 respiration fluxes

Mean total soil respiration values were consistent with those reported in other low-input agricultural systems across sub-Saharan Africa (Mapanda et al., 2010; Pelster et al., 2017; Rosenstock et al., 2016). In full sun (FS), the mean respiration (1.0 ± 0.9 g C-CO_2 m^{-2} d^{-1}) closely matched values measured by Wachiye et al. (2020) in a semi-arid Kenyan field at 1158 m altitude (1.1 ± 0.1 g C-CO_2 m^{-2} d^{-1}). This similarity likely reflects comparable environmental conditions, including moderate rainfall (~550 mm yr^{-1}) and low soil organic carbon and nitrogen contents (<1%) in the 0–20 cm layer of sandy soil. In contrast, respiration under *F. albida* canopy (Sh: 1.6 ± 1.1 g C-CO_2 m^{-2} d^{-1}) was higher, likely due to additional autotrophic respiration from tree roots and greater organic inputs beneath the canopy. Nonetheless, this flux remains close to values observed in low-input sorghum fields on sandy loam soils in eastern Ghana (1.7 ± 1.1 g C-CO_2 m^{-2} d^{-1}), despite higher rainfall (950–1000 mm yr^{-1}) in that region (Owusu et al., 2024).

Cumulative annual respiration fluxes fell within the range reported for Sahelian croplands (250–450 g C-CO_2 m^{-2}) (Brümmer et al., 2009) and other sub-Saharan African agricultural systems (Kim et al., 2016). The cumulative flux under tree cover is similar to that measured in cassava fields in

eastern Tanzania (440 g C-CO_2 m^{-2} yr^{-1}), despite the latter receiving higher rainfall (~1115 mm yr^{-1}) (Rosenstock et al., 2016). This convergence may stem from comparable soil fertility constraints, with low soil organic carbon (1–1.7%) and nitrogen contents (<0.5%). In contrast, the slightly lower cumulative flux in FS may reflect less favourable microclimatic conditions—such as elevated soil temperatures and increased aridity away from tree cover—limiting microbial activity (see Section 4.1).

Across sub-Saharan Africa, soil respiration fluxes based on static chamber measurements show high spatial variability, largely shaped by climate and land use. For example, Owusu et al. (2024) found higher respiration in woodlands (3.8 ± 0.8 g C-CO_2 m^{-2} d^{-1}) and grazed areas (2.7 ± 1.7) than in croplands (1.7 ± 1.1) in humid eastern Ghana. This gradient was linked to differences in soil moisture and organic matter. Similarly, Rosenstock et al. (2016) reported much higher fluxes in highland pastures in Kenya (3.8–4.4 g C-CO_2 m^{-2} d^{-1}) compared to cultivated fields in eastern Tanzania (1.2 ± 0.2), highlighting the role of vegetation cover and soil fertility.

4.4. Effect of trees on chamber-based soil respiration and photosynthesis

A notable increase in respiration and photosynthesis fluxes was observed under *F. albida* trees (Sh) compared at a distance from trees (FS). This increase may indicate the potential role of *F. albida* in modulating CO_2 exchange dynamics (Rch and GPPch) within this agro-silvo-pastoral system. These results are consistent with preliminary findings from similar environments (Duthoit et al., 2020).

Numerous studies have investigated the effect of tree species on greenhouse gas fluxes, particularly CO_2, revealing significant variations across different ecological contexts (Bréchet et al., 2021, 2025; Klaus et al., 2024; Mazza et al., 2021; Ramesh et al., 2013; Rheault et al., 2024). However, the underlying mechanisms by which trees influence these dynamics are not yet fully understood.

In general, agroforestry systems have been well-documented for their ability to provide a range of ecosystem services (e.g., Assefa et al., 2024; Bado et al., 2021; Kuyah et al., 2019; Rolo et al., 2023). Specifically, *Faidherbia*-based agroforestry systems may play a crucial role in regulating CO_2 exchanges between the soil and atmosphere. *F. albida*-based agroforestry systems are recognized for enhancing both soil organic and mineral fertility (Bayala et al., 2020; Dilla et al., 2019; Sileshi, 2016; Sileshi et al., 2020; Stephen et al., 2020), mainly through litter accumulation and direct inputs from livestock excreta under their canopies. Additionally, the extensive root system of *F. albida* trees helps concentrate mineral nutrients, contributing to the formation of a 'fertile island' effect under the trees (Siegwart et al., 2022; Eldridge et al., 2024). Moreover, *F. albida* improve water infiltration (Diongue et al., 2023; Faye et al., 2020; Sarr et al., 2023), enhance soil moisture retention (Clermont-Dauphin et al., 2023) and contribute to reduced soil

temperatures (de Carvalho et al., 2021; Lopes et al., 2024; Sida et al., 2018). These changes foster a more favourable environment for soil microbial activity and crop development (Diack et al., 2024; Diene et al., 2024; Leroux et al., 2020; Roupsard et al., 2020) under the trees compared to open areas. Consequently, this likely explains the stronger effect of soil moisture and the leaf area index of groundnuts on Rch under the trees, resulting in higher total respiration (Table 2). For photosynthesis, the effect of these parameters was similar in both FS and Sh (Table 2). However, the significantly higher intensity of GPPch under Sh can be explained by greater light use efficiency (α) and a higher maximum CO_2 uptake rate at light saturation (β) in this shaded environment. In agroforestry systems, light use efficiency can at least partially mitigate the reduction in photosynthetically active radiation under tree canopies (Charbonnier et al., 2017).

Similar results have been observed in different climatic conditions and ecosystems. Gomes et al. (2016) investigated soil respiration using mobile chambers (LI-8100-102 model) under trees in coffee-based agroforestry systems and in the open areas in Minas Gerais, Brazil. These studies were conducted with agroecological management practices, such as weeding, intercropping maize between coffee rows, and mulching. The agroforestry systems exhibited lower air and soil temperatures (at 5 and 10 cm depth) and higher air and soil humidity compared to the open areas (Gomes et al., 2016). These authors observed greater spatial variability in soil respiration in agroforestry system (34.1%) compared to the open areas (24.2%). This variability was mainly linked with fluctuations in labile carbon and total nitrogen, reflecting more favourable soil microclimate for microbial activity in agroforestry system. In contrast, soil temperature (10 cm depth) accounted for most of the variability observed in the open areas, where the absence of tree canopy resulted in high soil temperatures and low soil moisture (Gomes et al., 2016). Likewise, Haren et al. (2010) reported 38% higher soil respiration near large trees (DBH $>$ 35 cm) in clay-rich Amazonian forests compared to open sites. Interestingly, the magnitude of CO_2 fluxes was independent of tree species, indicating that canopy effects may outweigh species-specific traits in some contexts. In our study, *F. albida*'s influence on CO_2 fluxes aligns with this general pattern observed in tropical agroforestry. However, the mechanisms linking individual tree species to microbial and physicochemical drivers of CO_2 dynamics remain insufficiently understood and warrant further investigation (Jevon et al., 2023).

4.5. Birch Effect

A rapid increase in soil respiration was observed following the first rainfall events, particularly under *F. albida*. This phenomenon can be attributed to the lower bulk density of the soil under the trees (Clermont-Dauphin et al., 2023; Siegwart et al., 2023), which potentially lead to CO_2 accumulation during the dry season due to higher soil organic matter (SOM) (Siegwart et al., 2023). Additionally, the sensitivity of microbial communities to subtle variations in soil moisture,

compounded by the tree effect, may further explain this phenomenon, as outlined in Sections 4.1 and 4.3. This phenomenon, known as the 'Birch effect' (Birch, 1958), has been reported across various semi-arid ecosystems in sub-Saharan Africa (Ago et al., 2016b; Fan et al., 2015; Wieckowski et al., 2024), as well as other semi-arid ecosystems globally (Roby et al., 2022; Yan et al., 2014; Yu et al., 2020). In these contexts, the 'Birch effect' may result from the displacement of soil gas phases by the piston effect generated during water infiltration (Singh et al., 2023). Furthermore, microbial communities in semi-arid environments adopt osmoregulatory mechanisms to withstand water deficit (Warren, 2014), which is particularly pronounced during the dry season. This phenomenon reduces soil microbial metabolism (Schimel et al., 2007). Upon rapid soil rewetting, especially after prolonged dry periods, soil microbial metabolism process is swiftly reactivated, leading to a transient pulse in respiration and a CO_2 release (Barnard et al., 2020; Kim et al., 2012; Manzoni et al., 2020; Vargas et al., 2018). Isotopic signatures of soil respiration provide evidence supporting the hypothesis that these pulses result from the rapid mineralisation of necromass or osmolytes excreted by microorganisms under drought stress (Schimel et al., 2007; Unger et al., 2010). Additional factors may amplify the 'Birch effect'. For instance, drying-rewetting cycles can induce physical disruption of soil aggregates, enhance oxygen penetration and thereby expose previously protected organic matter to microbial decomposition (Rabbi et al., 2024). This increases substrate availability and subsequently boosts soil respiration fluxes.

The magnitude of the 'Birch effect' is modulated by the severity and duration of drought. Thus, at our study site, given the 8- to 9-month-long dry season, the 'Birch effect' is particularly intense. Indeed, extended drought periods promote greater accumulation of microbial necromass and intensify hypo-osmotic stress responses upon rewetting (Singh et al., 2023).

4.6. Comparing EC and chamber-based methods

Results revealed high seasonal variability, with higher values during the rainy season compared to the dry season. This seasonal pattern aligns with findings from studies in the Sahel using the EC method for CO_2 flux measurements (Brümmer et al., 2008; Tagesson et al., 2015; Agbohessou et al., 2023, Wieckowski et al., 2024). Comparable patterns have also been documented at the ecosystem scale in other semi-arid environments (Ago et al., 2014; Archibald et al., 2009; Ardö et al., 2008; Jia et al., 2020; Quansah et al., 2015; Williams et al., 2009; Zhang, Bi, et al., 2024).

Several comparative studies between chamber and EC methods have reported both congruent and divergent CO_2 flux estimates (Bastviken et al., 2022; Poyda et al., 2017; Riederer et al., 2014; Tang et al., 2008; Wang et al., 2010). In the present study, ecosystem respiration fluxes during the rainy season exhibited notable discrepancies measurements between EC (Reco.EC) and upscaled chamber-based (Rch.stand). This is attributable to differences in the flux components captured

by each method. Specifically, Reco.EC included respiration from below- and above-ground tree parts, crops (groundnuts and cowpeas), weeds, and soil, whereas Rch.stand accounted only respiration from below-ground tree, groundnut crop, and soil. Therefore, as expected, Reco.EC (4.6 ± 3.2 g C-CO_2 m^{-2} d^{-1}) were significantly higher than Rch.stand (2.0 ± 1.1 g C-CO_2 m^{-2} d^{-1}). For chamber-based GPP measurements, values were standardised (GPP-stand) by the field leaf area index (LAI.field). This allowed it to improve comparability with GPP.EC when trees were leafless in the rainy season. In both cases, GPP accounted only for crops (groundnut and cowpea) and weeds, as trees were non-photosynthetic in the rainy season. Despite this standardisation, GPP.EC values (-5.1 ± 3.6 g C-CO_2 m^{-2} d^{-1}) were significantly higher than GPPch.stand values (-4.2 ± 4.3 g C-CO_2 m^{-2} d^{-1}). However, no divergence was observed in August, and the intensity of the peak of GPP in September was similar in both methods, but from the onset of groundnut senescence, when weeds became the dominant photosynthetic contributors. Thus, during the groundnut growth season, with leafless *F. albida* trees and almost no weeds, GPP measurements from EC and chambers generate closely comparable results. Therefore, this provides an initial form of cross-validation between the two methods. It is important to note that the EC method integrates CO_2 fluxes over a larger spatial scale, encompassing all ecosystem components (Baldocchi, 2003), while the chamber method captures fluxes on a smaller scale (i.e., at the 0.25 m^2 scale). This scale disparity can introduce uncertainties when upscaling chamber-based fluxes to the field, as vegetation composition within chambers does not represent the EC footprint average vegetation. This makes upscaling chamber-based measurements challenging. Nevertheless, the standardisation we applied on chamber photosynthesis by LAI has been relatively successful.

During the dry season, Reco.EC included respiration from below- and above-ground tree parts (with leaves) and bare soil, while Rch.stand measured only below-ground tree and bare soil respiration. Consequently, the difference between Reco.EC and Rch.stand was solely attributable to above-ground tree respiration (Ra tree above-ground). In terms of GPP, chamber measurements were nil, whereas GPP.EC reflected only GPP trees.

The transition period, characterised by groundnut senescence, tree leaf regrowth, and weed proliferation, introduced further complexity, amplifying method-specific discrepancies. Rch.stand measurements facilitated the estimation of tree contribution to Reco.EC (Ra tree) and the verification of the consistency for EC results in terms of carbon use efficiency (CUE), estimated here at 0.48. This value indicates that nearly 50% of the carbon captured by trees is allocated to biomass. The CUE estimate here is well comparable to the global average across diverse ecosystems, climates, and management practices (0.49 ± 0.14) (Tang et al., 2019). Similar CUE values have been reported for semi-arid grasslands (0.46 ± 0.10), but our value is notably lower than those documented for wetlands (0.61 ± 0.13) (Tang et al., 2019). Overall, these findings

reinforce the plausibility of our assumptions regarding the compartment contributions to Reco.EC and Rch.stand, thereby providing a second cross-validation of the EC-Ch comparison. However, despite a frequently assumed CUE of 0.5 in models, global estimates span a broad range (0.20 to 0.82), depending on ecosystem type and management practices (DeLucia et al., 2007; Tang et al., 2019). This underscores the importance of refining carbon flux models to better represent the biophysical processes governing CO_2 exchange in semi-arid agroforestry systems. The combined use of EC and chamber methodologies offers a comprehensive perspective on ecosystem-scale CO_2 flux dynamics, advancing the understanding of carbon cycling in these environments.

4.7. Net annual vertical carbon balance

The net annual carbon balance was quantified at -1.4 $\pm$ 0.46 Mg C-CO_2 ha^{-1} with the chamber method and -1.8 $\pm$ 0.17 Mg C-CO_2 ha^{-1} by the Eddy Covariance (EC), indicating that the studied agro-silvo-pastoral system functions as a net carbon sink. These findings corroborate the system potential role in mitigating greenhouse gas emissions, consistent with previous studies reporting vertical CO_2 flux balances in semi-arid ecosystems (Rahimi et al., 2021; Tagesson et al., 2015; Agbohessou et al., 2023, Wieckowski et al., 2024).

The estimated net C exchange balance is close to the reported mean for Sahelian ecosystems (-1.6 $\pm$ 0.5 Mg C-CO_2 ha^{-1}; Tagesson et al., 2016). The EC-based net C exchange balance (-1.8 $\pm$ 0.17 Mg C-CO_2 ha^{-1}) is also similar to the value of -1.9 $\pm$ 0.4 Mg C-CO_2 ha^{-1} reported for semi-arid savannas of northeastern Benin, despite higher annual rainfall (1495 mm; Ago et al., 2016b). Furthermore, our EC estimate is close to the average net C exchange reported for West African terrestrial ecosystems (-2.0 $\pm$ 1.5 Mg C-CO_2 ha^{-1}; Ago et al., 2016a).

However, estimates from Tagesson et al. (2015) (-2.7 $\pm$ 0.07 Mg C-CO_2 ha^{-1}) for a semi-arid savannah in Dahra, Senegal, located between the 300 mm and 400 mm isohyets, were comparatively higher. This is potentially attributable to specific characteristics of that specific savannah site, such as herbaceous vegetation cover during the rainy season, the presence of evergreen trees, and land management practices linked to pastoral livestock activities (Tagesson et al., 2016).

The net annual C balance estimates presented in this study are, in fact, representing vertical fluxes only, given that they exclude organic matter (OM) imports and, more critically, exports, introducing uncertainties. Notably, the export of crop residues and direct inputs from animal excreta —particularly significant in 'bush fields' during the dry season — were not accounted for. In our case of 'bush field', crop residues are exported to feed livestock, while livestock faeces are collected for use as fuel or manure in 'home fields'. Such practices may lead to a significant soil organic carbon stocks depletion (Malou et al, 2021), potentially diminishing the net C budget (-

797 1.4 ± 0.46 Mg C-CO_2 ha^{-1}) over time and shifting the system closer to carbon neutrality (Assouma
798 et al., 2019).
799 These results should be contextualized within the broader framework of climate change and semi-
800 arid ecosystem management. Although agro-silvo-pastoral systems can function as apparent
801 annual carbon sinks, they remain highly sensitive to interannual rainfall variability and escalating
802 anthropogenic pressures. Sustainable management practices, particularly regarding C
803 inputs/outputs from the system regarding crop harvest, residues exportation, and cattle free
804 manuring, must be taken into account to confirm the capacity of the system to act as effective a
805 carbon sink.

806 *4.8. Limitations of the study*

807 This study benefited from the inverse phenology of *F. albida*, allowing for direct comparison
808 between chamber-based GPP (GPPch.stand) and ecosystem-level GPP (GPP.EC) during the
809 leafless period of the trees. However, the system spatial heterogeneity —common in
810 agroforestry— posed challenges for accurately partitioning CO_2 fluxes among trees, crops, and
811 soil. A key limitation was the development of weeds during the late rainy season, which
812 complicated the attribution of fluxes, particularly during the transitional period. Additionally,
813 while GPPch was successfully standardised by LAI for upscaling, this was not feasible for
814 respiration. Respiration integrates both autotrophic and heterotrophic components, which
815 respond to different drivers and are not directly linked to LAI, limiting the precision of upscaled
816 Rch.
817 Future improvements should aim to separately quantify respiration sources —tree roots, crops,
818 and microbial (heterotrophic) respiration— and account explicitly for the weed layer, to refine
819 flux partitioning in such complex agroforestry systems.
820 Furthermore, the present study constitutes only an intermediate step delivering a first integrated
821 estimate of the main vertical CO_2 exchanges (photosynthesis, respiration, and net ecosystem
822 exchange) as a base for a forthcoming paper that will present a more comprehensive carbon
823 budget of the ecosystem. Establishing such a carbon budget would require substantial additional
824 data acquisition and poses considerable methodological challenges. In particular, quantifying
825 carbon inputs/outputs associated with free-ranging livestock grazing would be difficult to achieve
826 with acceptable accuracy. It must also be recognised that the system is in a dynamic, non-steady
827 state, characterised by marked inter-annual variability as well as periods of carbon storage and
828 release, which are difficult to constrain empirically except through modeling.

Conclusion

This study demonstrates the successful application of automated dynamic chambers to quantify CO_2 fluxes in a Sahelian agroforestry system dominated by *F. albida*. The continuous, high-frequency measurements captured key seasonal dynamics and short-lived events (e.g., Birch effect), providing a more accurate assessment of carbon exchange than traditional intermittent sampling.

By integrating crop and soil components and applying dynamic partitioning models, the study quantified both respiration and photosynthesis fluxes at fine temporal resolution. The results revealed a clear 'fertile island' effect under tree canopies, with higher respiration and photosynthetic activity, and highlighted the significant contribution of F. albida trees to annual carbon uptake.

The consistency between chamber- and eddy covariance-based estimates reinforces the robustness of the methodology. Overall, this work underscores the role of *F. albida*-based agroforestry systems in the dynamic of C exchanges in semi-arid environments, offering valuable insights for carbon accounting and sustainable land management in the Sahel.

Acknowledgments

This research was financially supported by the CaSSECS project (Carbon Sequestration and Greenhouse Gas Emissions in (Agro) Silvopastoral Systems of the CILS-Sahel States (FOOD/2019/410-169), within the framework of the European Union's initiative 'Development of Smart Innovation through Agricultural Research' (DeSIRA-UE-EuropAID). We extend our sincere gratitude to the coordination team of the CaSSECS project, the ''Laboratoire Mixte International Intensification Écologique des Sols Cultivés en Afrique de l'Ouest'' (LMI IESOL) of the of the French National Institute for Development (IRD) in Dakar (Senegal), as well as to the Faidherbia-Flux platform (https://lped.info/wikiObsSN/?Faidherbia-Flux), its partners, and affiliated projects: EU-H2020 [SUSTAIN-SAHEL (Grant N° 861974)] ; ANR under the France 2030 program [PEPR FairCarboN-RIFT (reference ANR-22-PEXF-0004)]; EU-HORIZON EUROPE [GALILEO (Grant N° 101181623)]. Our deepest appreciation goes to Ibou Diouf, the observer at our experimental site. Tagesson also acknowledged funding from Formas (Dnr 2021-00644). Lastly, we are deeply grateful to the two reviewers, Riccardo Picone and Jim Boonman, for their insightful and highly constructive comments.

Author contribution: CRediT

Seydina Mohamad BA: Conducting in situ experiments, collecting and processing data, writing-original draft, review and editing. **Olivier Roupsard**: Designing experimental apparatus and methodology, writing, review and editing. **Lydie Chapuis-Lardy**: Designing methodology, writing, review and editing. **Yélognissè Agbohessou**: Processing data, review and editing. **Fred Bouvery**: Designing chambers and connection to the instrument, review and editing. **Maxime Duthoit**: Designing experimental set and methodology, review and editing. **Aleksander Wieckowski**: Review and editing. **Mohamed Habibou Assouma**: Review and editing. **Espoir Gaglo**: Processing data, review and editing. **Claire Delon**: review and editing. **Torbern Tagesson**: Designing methodology, review, and editing. **Bienvenu Sambou**: Review and editing. **Dominique Serça**: Designing methodology, writing, review and editing.

References

Agbohessou, Y., Delon, C., Mougin, E., Grippa, M., Tagesson, T., Diedhiou, M., Ba, S., Ngom, D., Vezy, R., Ndiaye, O., Assouma, M. H., Diawara, M., & Roupsard, O.: To what extent are greenhouse-gas emissions offset by trees in a Sahelian silvopastoral system?, Agr. Forest. Meteorl., 343, 109780, https://doi.org/10.1016/j.agrformet.2023.109780, 2023.

Agbohessou, Y., Delon, C., Grippa, M., Mougin, E., Ngom, D., Gaglo, E. K., Ndiaye, O., Salgado, P., and Roupsard, O.: Modelling CO_2 and N_2O emissions from soils in silvopastoral systems of the West African Sahelian band. Biogeosciences, 21, 2811–2837, https://doi.org/10.5194/bg-21-2811-2024, 2024.

Ago, E., Agbossou, K., Ozer, P., & Aubinet, M.: Mesure des flux de CO_2 et séquestration de carbone dans les écosystèmes terrestres ouest-africains (synthèse bibliographique), Biotechnologie, Biotechnol. Agron. Soc. Environ., 20(1), 68-82, https://doi.org/10.25518/1780-4507.12565, 2016a.

Ago, E., Agbossou, E. K., Cohard, J. M., Galle, S., & Aubinet, M.: Response of CO_2 fluxes and productivity to water availability in two contrasting ecosystems in northern Benin (West Africa), Ann. Forest. Sci., 73(2), 483-500, https://doi.org/10.1007/s13595-016-0542-9, 2016b.

Ago, E., Agbossou, E. K., Galle, S., Cohard, J. M., Heinesch, B., & Aubinet, M.: Long term observations of carbon dioxide exchange over cultivated savanna under a Sudanian climate in Benin (West Africa), Agr. Forest. Meteorl., 197, 13-25, https://doi.org/10.1016/j.agrformet.2014.06.005, 2014.

Archibald, S. A., Kirton, A., van der Merwe, M.R, Scholes, R. J., Williams, C.A, & Hanan, H.: Drivers of inter-annual variability in Net Ecosystem Exchange in a semi-arid savanna ecosystem, South Africa, Biogeosciences, 6, 251–266, https://doi.org/10.5194/bg-6-251-2009, 2009.

Ardö, J., Mölder, M., El-Tahir, B. A., & Elkhidir, H. A. M.: Seasonal variation of carbon fluxes in a sparse savanna in semi-arid Sudan, Carbon Balance and Manag., 3(1), 7, https://doi.org/10.1186/1750-0680-3-7, 2008.

Assefa, A., Muthuri, C. W., Gebrekirstos, A., Hadgu, K., & Fetene, M.: Tree growth and wheat productivity are affected by pollarding *Faidherbia albida* in semi-arid Ethiopia, Agroforest. Syst., 98(3), 783-796, https://doi.org/10.1007/s10457-023-00948-7, 2024.

Assouma, M. H., Hiernaux, P., Lecomte, P., Ickowicz, A., Bernoux, M., & Vayssières, J.: Contrasted seasonal balances in a Sahelian pastoral ecosystem result in a neutral annual carbon balance, J. Arid Environ., 162, 62-73, https://doi.org/10.1016/j.jaridenv.2018.11.013, 2019.

Assouma, M. H., Serça, D., Guérin, F., Blanfort, V., Lecomte, P., Touré, I., Ickowicz, A., Manlay, R. J., Bernoux, M., & Vayssières, J.: Livestock induces strong spatial heterogeneity of soil CO_2, N_2O and CH_4 emissions within a semi-arid sylvo-pastoral landscape in West Africa, J. Arid Land, 9(2), 210-221, https://doi.org/10.1007/s40333-017-0001-y, 2017.

Bado, B. V., Whitbread, A., & Sanoussi Manzo, M. L.: Improving agricultural productivity using agroforestry systems: Performance of millet, cowpea, and ziziphus-based cropping systems in West Africa Sahel, Agr. Ecosyst. Environ., 305, 107175, https://doi.org/10.1016/j.agee.2020.107175, 2021.

Bahn, M., Reichstein, M., Davidson, E. A., Grünzweig, J., Jung, M., Carbone, M. S., Epron, D., Misson, L., Nouvellon, Y., Roupsard, O., Savage, K., Trumbore, S. E., Gimeno, C., Curiel Yuste, J., Tang, J., Vargas, R., & Janssens, I. A.: Soil respiration at mean annual temperature predicts annual total across vegetation types and biomes, Biogeosciences, 7(7), 2147-2157, https://doi.org/10.5194/bg-7-2147-2010, 2010.

Baldocchi, D.: Assessing the eddy covariance technique for evaluating carbon dioxide exchange rates of ecosystems: Past, present and future, Glob. Change Biol., 9, 479-492, https://doi.org/10.1046/j.1365-2486.2003.00629.x, 2003.

Baldocchi, D.: « Breathing » of the terrestrial biosphere: Lessons learned from a global network of carbon dioxide flux measurement systems, Aust. J. Bot., 56(1), 1, https://doi.org/10.1071/BT07151, 2008.

Baldocchi, D.: How eddy covariance flux measurements have contributed to our understanding of global change biology, Glob. Change Biol., 26: 242–260, https://doi.org/10.1111/gcb.14807, 2020.

Barnard, R. L., Blazewicz, S. J., & Firestone, M. K.: Rewetting of soil: Revisiting the origin of soil CO_2 emissions, Soil Biol. Biochem., 147, https://doi.org/10.1016/j.soilbio.2020.107819, 2020.

Bastviken, D., Wilk, J., Duc, N. T., Gålfalk, M., Karlson, M., Neset, T.-S., Opach, T., Enrich-Prast, A., & Sundgren, I.: Critical method needs in measuring greenhouse gas fluxes. Environ. Res. Lett., 17(10), 104009, https://doi.org/10.1088/1748-9326/ac8fa9, 2022.

Bayala, J., Sanou, J., Bazié, H. R., Coe, R., Kalinganire, A., & Sinclair, F. L.: Regenerated trees in farmers' fields increase soil carbon across the Sahel, Agroforest. Syst., 94(2), 401-415, https://doi.org/10.1007/s10457-019-00403-6, 2020.

Birch, H. F.: The effect of soil drying on humus decomposition and nitrogen availability, Plant and Soil, 10(1), 9-31, https://doi.org/10.1007/BF01343734, 1958.

Bombelli A, Henry M., Castaldi S., Adu-Bredu S, Arneth A, De Grandcourt A, Grieco E., Kutsch W.L., Lehsten V., Rasile A., Reichstein M, Tansey K., Weber U, Valentini R.: An outlook on the Sub-Saharan Africa carbon balance, Biogeosciences, 6 (10), 2193-2205, https://doi.org/10.5194/bg-6-2193-2009, 2009.

Borken, W., Xu, Y., Davidson, E. A., & Beese, F.: Site and temporal variation of soil respiration in European beech, Norway spruce, and Scots pine forests, Glob. Change Biol., 8(12), 1205-1216, https://doi.org/10.1046/j.1365-2486.2002.00547.x, 2002.

Bréchet, L. M., Daniel, W., Stahl, C., Burban, B., Goret, J. Y., Salomón, R. L., & Janssens, I. A.: Simultaneous tree stem and soil greenhouse gas (CO_2, CH_4, N_2O) flux measurements: A novel design for continuous monitoring towards improving flux estimates and temporal resolution, New Phytol., 230(6), 2487-2500, https://doi.org/10.1111/nph.17352, 2021.

Bréchet, L. M., Salomón, R. L., Machacova, K., Stahl, C., Burban, B., Goret, J. Y., Steppe, K., Damien, B., & Janssens, I. A.: Insights into the sub daily variations in methane, nitrous oxide and carbon dioxide fluxes from upland tropical tree stems, New Phytol., 20401, https://doi.org/10.1111/nph.20401, 2025.

Brümmer, C., Falk, U., Papen, H., Szarzynski, J., Wassmann, R., & Brüggemann, N.: Diurnal, seasonal, and interannual variation in carbon dioxide and energy exchange in shrub savanna in Burkina Faso (West Africa), Biogeosciences, 113, G2030, https://doi.org/10.1029/2007JG000583, 2008.

Brümmer, C., Papen, H., Wassmann, R., & Brüggemann, N.: Fluxes of CH_4 and CO_2 from soil and termite mounds in south Sudanian savanna of Burkina Faso (West Africa), Global Biogeochem. Cycles, 23, GB1001, https://doi.org/10.1029/2008GB003237, 2009.

Cardinael, R., Cadisch, G., Gosme, M., Oelbermann, M., & Van Noordwijk, M.: Climate change mitigation and adaptation in agriculture: Why agroforestry should be part of the solution? Agr. Ecosyst. Environ., 319, 107555, https://doi.org/10.1016/j.agee.2021.107555, 2021.

Charbonnier, F., Roupsard, O., le Maire, G., Guillemot, J., Casanoves, F., Lacointe, A., Vaast, P., Allinne, C., Audebert, L., Cambou, A., Clément-Vidal, A., Defrenet, E., Duursma, R. A., Jarri, L., Jourdan, C., Khac, E., Leandro, P., Medlyn, B. E., Saint-André, L., Thaler, P., Van Den Meersche, K., Barquero Aguilar, A., Lehner, P., & Dreyer, E.: Increased light-use efficiency sustains net primary productivity of shaded coffee plants in agroforestry system, Plant Cell and Environ., 40(8), 1592-1608, https://doi.org/10.1111/pce.12964, 2017.

Chu, H., Luo, X., Ouyang, Z., et al.: Representativeness of Eddy-Covariance flux footprints for areas surrounding AmeriFlux sites, Agr. Forest. Meteorol., 301-302, 108350, https://doi.org/10.1016/j.agrformet.2021.108350, 2021.

Clermont-Dauphin, C., N'dienor, M., Leroux, L., Ba, Halimatou. S., Bongers, F., Jourdan, C., Roupsard, O., Do, F. C., Cournac, L., & Seghieri, J.: *Faidherbia albida* trees form a natural buffer against millet water stress in agroforestry parklands in Senegal, Biotechnol. Agron. Soc. Environ, 182-195, https://doi.org/10.25518/1780-4507.20477, 2023.

Conant, R. T., Dalla-Betta, P., Klopatek, C. C., & Klopatek, J. M.: Controls on soil respiration in semiarid soils, Soil Biol. Biochem., 36(6), 945-951, https://doi.org/10.1016/j.soilbio.2004.02.013, 2004.

Crosson, E.: A cavity ring-down analyzer for measuring atmospheric levels of methane, carbon dioxide, and water vapor, App. Phys. B-Lasers O., 92, 403-408, https://doi.org/10.1007/s00340-008-3135-y, 2008.

de Carvalho, A. F., Fernandes-Filho, E. I., Daher, M., Gomes, L. de C., Cardoso, I. M., Fernandes, R. B. A., & Schaefer, C. E. G. R.: Microclimate and soil and water loss in shaded and unshaded agroforestry coffee systems, Agroforest. Syst., 95(1), 119-134, https://doi.org/10.1007/s10457-020-00567-6, 2021.

Delon, C., Galy-Lacaux, C., Serça, D., Personne, E., Mougin, E., Adon, M., ... & Tagesson, T.: Modelling land–atmosphere daily exchanges of NO, NH_3, and CO_2 in a semi-arid grazed ecosystem in Senegal, Biogeosciences, 16(9), 2049-2077, https://doi.org/10.5194/bg-16-2049-2019, 2019.

Delaunay, V., Desclaux, A., & Sokhna, Ch.: Niakhar, mémoires et perspectives : Recherches pluridisciplinaires sur le changement en Afrique, IRD Éditions/L'Harmattan, 536 p., ISBN 9782140103551, 2140103556 https://www.editions.ird.fr/open_access_download/851/441, 2019.

988 DeLucia, E. H., Drake, J. E., Thomas, R. B., & Gonzalez-Meler, M.: Forest carbon use efficiency: Is
989 respiration a constant fraction of gross primary production?, Glob. Change Biol., 13(6),
990 1157-1167, https://doi.org/10.1111/j.1365-2486.2007.01365.x, 2007.

991 Denmead, O. T.: Approaches to measuring fluxes of methane and nitrous oxide between
992 landscapes and the atmosphere, Plant and Soil, 309(1-2), 5-24, https://doi.org/10.1007/s11104-
993 008-9599-z, 2008.

994 Diack, I., Diene, S., Leroux, L., Diouf, A., Benjamin, H., Olivier, R., Letourmy, P., Alain, A., Sarr, I., &
995 Moussa, D.: Combining UAV and Sentinel-2 Imagery for Estimating Millet FCover in a
996 Heterogeneous Agricultural Landscape of Senegal, IEEE J. Sel. Top. Appl. Earth Obs. Remote Sens.,
997 17, 7305-7322, https://doi.org/10.1109/JSTARS.2024.3373508, 2024.

998 Diene, S. M., Diack, I., Audebert, A., Roupsard, O., Leroux, L., Diouf, A. A., Mbaye, M., Fernandez, R.,
999 Diallo, M., Sarr, I.: Improving pearl millet yield estimation from UAV imagery in the semiarid
1000 agroforestry system of Senegal through textural indices and reflectance normalization, in IEEE
1001 Access, 12, 132626-132643, https://doi.org/10.1109/ACCESS.2024.3460107, 2024.

1002 Dilla, A. M., Smethurst, P. J., Barry, K., & Parsons, D.: Preliminary estimate of carbon sequestration
1003 potential of *Faidherbia albida* (Delile) A. Chev in an agroforestry parkland in the Central Rift Valley
1004 of Ethiopia, For. Trees Livelihoods, 28(2), 79-89,
1005 https://doi.org/10.1080/14728028.2018.1564146, 2019.

1006 Diongue, D., Brunetti, G., Stumpp, C., Do, F., Roupsard, O., Orange, D., Faye, W., Sow, S., Jourdan, C.,
1007 & Faye, S.: A Probabilistic Framework for Assessing the Hydrological Impact of *Faidherbia albida*
1008 in an Arid Area of Senegal, J. Hydrol., 622, 129717,
1009 https://doi.org/10.1016/j.jhydrol.2023.129717, 2023.

1010 Diongue, D. M. L., Roupsard, O., Do, F. C., Stumpp, C., Orange, D., Sow, S., Jourdan, C., & Faye, S.:
1011 Evaluation of parameterisation approaches for estimating soil hydraulic parameters with
1012 HYDRUS-1D in the groundnut basin of Senegal, Hydrol. Sci. J., 67(15), 2327–2343,
1013 https://doi.org/10.1080/02626667.2022.2142474, 2022.

1014 Duthoit, M., Roupsard, O., Créquy, N., & Sauze, J.: Conception d'un dispositif automatisé de
1015 chambres de mesures d'échanges gazeux du sol à fermeture horizontale, Le Cahier des Techniques
1016 de l'Inra, 102, 19 p., hal-03989886, https://hal.science/hal-03989886/document, 2020.

Eldridge, D.J., Ding, J., Dorrough, J. et al. Hotspots of biogeochemical activity linked to aridity and plant traits across global drylands. Nat. Plants 10, 760–770 (2024). https://doi.org/10.1038/s41477-024-01670-7

Evans, S., Dieckmann, U., Franklin, O., & Kaiser, C.: Synergistic effects of diffusion and microbial physiology reproduce the Birch effect in a micro-scale model, Soil Biol. Biochem., 93, 28-37, https://doi.org/10.1016/j.soilbio.2015.10.020, 2016.

Falge, E., Baldocchi, D., Olson, R., Anthoni, P., Aubinet, M., Bernhofer, C., Burba, G., Ceulemans, R., Clement, R., Dolman, H., Granier, A., Gross, P., Grünwald, T., Hollinger, D., Jensen, N.-O., Katul, G., Keronen, P., Kowalski, A., Ta Lai, C., … Oren, R.: Gap filling strategies for defensible annual sums of net ecosystem exchange, Agr. Forest Meteorol., 107, 43-69, https://doi.org/10.1016/S0168-1923(00)00225-2, 2001.

Fan, Z., Neff, J. C., & Hanan, N. P.: Modeling pulsed soil respiration in an African savanna ecosystem, Agr. Forest Meteorol., 200, 282-292, https://doi.org/10.1016/j.agrformet.2014.10.009, 2015.

Fang, F., Han, X., Liu, W., & Tang, M.: Carbon dioxide fluxes in a farmland ecosystem of the southern Chinese Loess Plateau measured using a chamber-based method, PeerJ, 8, 8994, https://doi.org/10.7717/peerj.8994, 2020.

Faye, W., Fall, A. N., Orange, D., Do, F., Roupsard, O., & Kane, A.: Climatic variability in the Sine-Saloum basin and its impacts on water resources: Case of the Sob and Diohine watersheds in the region of Niakhar, Proceedings of the International Association of Hydrological Sciences, 383, 391-399, https://doi.org/10.5194/piahs-383-391-2020, 2020.

Finkelstein, P. L., & Sims, P. F.: Sampling error in eddy correlation flux measurements, J. Geophys. Res., 106(D4), 3503–3509, https://doi.org/10.1029/2000JD900731, 2001.

Fleck, D., He, Y., Alexander, C., Jacobson, G., & Cunningham, K. L.: Simultaneous soil flux measurements of five gases-N_2O, CH_4, CO_2, NH_3, and H_2O-with the Picarro G2508," Picarro Application Note, AN034, https://www.picarro.com/sites/default/files/product_documents/Picarro_AN034_Soil%20Flux%20with%20the%20G2508_1.pdf, 2013.

Foken, T., Göockede, M., Mauder, M., Mahrt, L., Amiro, B., Munger, W.: Post-Field Data Quality Control, In: Lee, X., Massman, W., Law, B. (eds) Handbook of Micrometeorology, Atmos. Ocean. Sci. Lib., vol 29, Springer, Dordrecht, https://doi.org/10.1007/1-4020-2265-4_9, 2004.

1047 Foken, T., Aubinet, M., & Leuning, R.: Eddy Covariance. In M. Aubinet, T. Vesala, & D. Papale (eds),
1048 Eddy Covariance, p.1-19, Springer, Netherlands, https://doi.org/10.1007/978-94-007-2351-1,
1049 2012.

1050 Fox, J., Weisberg, S., & Price, B.: car: Companion to Applied Regression (version 3.1-3) [Dataset].
1051 https://doi.org/10.32614/CRAN.package.car, 2023.

1052 Gomes, L. D. C., Cardoso, I. M., Mendonça, E. D. S., Fernandes, R. B. A., Lopes, V. S., & Oliveira, T. S.:
1053 Trees modify the dynamics of soil CO_2 efflux in coffee agroforestry systems, Agr. Forest. Meteorol.,
1054 224, 30-39, https://doi.org/10.1016/j.agrformet.2016.05.001, 2016.

1055 Gonsamo, A., Chen, J. M., He, L., Sun, Y., Rogers, C., & Liu, J.: Exploring SMAP and OCO-2 observations
1056 to monitor soil moisture control on photosynthetic activity of global drylands and croplands,
1057 Remote Sens. Environ., 232, 111314, https://doi.org/10.1016/j.rse.2019.111314, 2019.

1058 Guillen-Cruz, G., Campuzano, E. F., Juárez-Altamirano, R., López-García, K. L., Torres-Arreola, R., &
1059 Flores-Rentería, D.: Interannual Variation and Control Factors of Soil Respiration in Xeric
1060 Shrubland and Agricultural Sites from the Chihuahuan Desert, Mexico, Land, 12(11), 1961,
1061 https://doi.org/10.3390/land12111961, 2023.

1062 Gupta, S.R., Dagar, J.C., Sileshi, G.W., Chaturvedi, R.K.: Agroforestry for Climate Change Resilience
1063 in Degraded Landscapes. In: Dagar, J.C., Gupta, S.R., Sileshi, G.W. (eds) Agroforestry for Sustainable
1064 Intensification of Agriculture in Asia and Africa, Sustain. Sci. in Asia Afr., Springer, Singapore.
1065 https://doi.org/10.1007/978-981-19-4602-8_5, 2023.

1066 Houghton, R. A. and Hackler, J. L.: Emissions of carbon from land use change in sub-Saharan Africa,
1067 Geophys. Res., 111, G02003, https://doi.org/10.1029/2005JG000076, 2006.

1068 IUSS Working Group WRB.: World Reference Base for Soil Resources. International soil
1069 classification system for naming soils and creating legends for soil maps, 4th edition, International
1070 Union of Soil Sciences (IUSS), Vienna, Austria, ISBN 979-8-9862451-1-9,
1071 www.isric.org/sites/default/files/WRB_fourth_edition_2022-12-18.pdf, 2022.

1072 Jackson, R.B., Canadell, J., Ehleringer, J.R. et al.: A global analysis of root distributions for terrestrial
1073 biomes, Oecologia 108, 389–411, https://doi.org/10.1007/BF00333714, 1996.

1074 Jevon, F. V., Gewirtzman, J., Lang, A. K., Ayres, M. P., & Matthes, J. H.: Tree Species Effects on Soil
1075 CO_2 and CH_4 Fluxes in a Mixed Temperate Forest, Ecosystems, 26(7), 1587-1602,
1076 https://doi.org/10.1007/s10021-023-00852-2, 2023.

Jia, X., Mu, Y., Zha, T., Wang, B., Qin, S., & Tian, Y.: Seasonal and interannual variations in ecosystem respiration in relation to temperature, moisture, and productivity in a temperate semi-arid shrubland, Sci. Total Environ., 709, 136210, https://doi.org/10.1016/j.scitotenv.2019.136210, 2020.

Juszczak, R., Acosta, M., Olejnik, J.: Comparison of Daytime and Nighttime Ecosystem Respiration Measured by the Closed Chamber Technique on a Temperate Mire in Poland, *Pol. J. Environ. Stud.* Vol. 21, No. 3, 643-658, 2012.

Kim, D. G., Vargas, R., Bond-Lamberty, B., & Turetsky, M. R.: Effects of soil rewetting and thawing on soil gas fluxes: A review of current literature and suggestions for future research, Biogeosciences, 9(7), 2459-2483, https://doi.org/10.5194/bg-9-2459-2012, 2012.

Kim, D.-G., Thomas, A. D., Pelster, D., Rosenstock, T. S., & Sanz-Cobena, A.: Greenhouse gas emissions from natural ecosystems and agricultural lands in sub-Saharan Africa: Synthesis of available data and suggestions for further research, Biogeosciences, 13(16), 4789-4809, https://doi.org/10.5194/bg-13-4789-2016, 2016.

Klaus, M., Öquist, M., & Macháčová, K.: Tree stem-atmosphere greenhouse gas fluxes in a boreal riparian forest, Sci. Total Environ., 954, 176243. https://doi.org/10.1016/j.scitotenv.2024.176243, 2024.

Kormann, R., & Meixner, F. X.: An analytical footprint model for non-neutral stratification, Boundary-Layer Meteorol., 99, 207-224, https://doi.org/10.1023/A:1018991015119, 2001.

Kuyah, S., Whitney, C. W., Jonsson, M., Sileshi, G. W., Öborn, I., Muthuri, C. W., & Luedeling, E.: Agroforestry delivers a win-win solution for ecosystem services in sub-Saharan Africa. A meta-analysis, Agron. Sustain. Dev., 39(5), https://doi.org/10.1007/s13593-019-0589-8, 2019.

Lambers, H., Chapin, F. S., & Pons, T. L.: Plant Physiol. Ecol., Springer New York. https://doi.org/10.1007/978-0-387-78341-3, 2008.

Lasslop, G., Reichstein, M., Papale, D., Richardson, A., Arneth, A., Barr, A., Stoy, P., & Wohlfahrt, G.: Separation of net ecosystem exchange into assimilation and respiration using a light response curve approach: Critical issues and global evaluation, Glob. Change Biol., 16(1), 187-208. https://doi.org/10.1111/j.1365-2486.2009.02041.x, 2010.

Lembrechts J.J, Aalto J, Ashcroft MB, et al.: SoilTemp: A global database of near-surface temperature, Glob. Change Biol., 26, 6616–6629, https://doi.org/10.1111/gcb.15123, 2020.

1107 Lembrechts, J. J., van den Hoogen, J., Aalto, J., et al.: Global maps of soil temperature. Glob. Change
1108 Biol., 28, 3110-3144, https://doi.org/10.1111/gcb.16060, 2022.

1109 Leroux, L., Falconnier, G. N., Diouf, A. A., Ndao, B., Gbodjo, J. E., Tall, L., Balde, A. A., Clermont-
1110 Dauphin, C., Bégué, A., Affholder, F., & Roupsard, O.: Using remote sensing to assess the effect of
1111 trees on millet yield in complex parklands of Central Senegal, Agr. Syst., 184,
1112 https://doi.org/10.1016/j.agsy.2020.102918, 2020.

1113 Liu, W., Zhang, Z., & Wan, S.: Predominant role of water in regulating soil and microbial respiration
1114 and their responses to climate change in a semiarid grassland, Glob. Change Biol., 15(1), 184-195,
1115 https://doi.org/10.1111/j.1365-2486.2008.01728.x, 2009.

1116 Liu, Y., He, N., Wen, X., Xu, L., Sun, X., Yu, G., Liang, L., & Schipper, L. A.: The optimum temperature
1117 of soil microbial respiration: Patterns and controls, Soil Biol. Biochem., 121, 35-42,
1118 https://doi.org/10.1016/j.soilbio.2018.02.019, 2018.

1119 Lloyd, J., & Taylor, J. A.: On the Temperature Dependence of Soil Respiration, Funct. Ecol., 8(3),
1120 315-323, https://doi.org/10.2307/2389824,1994.

1121 Lopes, V. S., Cardoso, I. M., Cavalcante, V. S., Gomes, L. de C., Tanure, M. M. C., Moura, W. de M.,
1122 Mendonça, E. de S., & Fernandes, R. B. A.: Soil CO_2 efflux in coffee agroforestry and full-sun coffee
1123 systems, Acta Sci. – Agr, 46(1), e65877, https://doi.org/10.4025/actasciagron.v46i1.65877,
1124 2024.

1125 Lüdecke, D., Ben-Shachar, M., Patil, I., Waggoner, P., & Makowski, D.: Performance: An R Package
1126 for Assessment, Comparison and Testing of Statistical Models, J. Open Source Softw., 6(60), 3139,
1127 https://doi.org/10.21105/joss.03139, 2021.

1128 Luo, Y., & Zhou, X.: Methods of Measurements and Estimations. In Y. Luo & X. Zhou (eds) Soil
1129 Respiration and Environment, 161-185 p., Academic Press, Elsevier,
1130 https://doi.org/10.1016/B978-0-12-088782-8.X5000-1, 2006.

1131 Macharia, J. M., Pelster, D. E., Ngetich, F. K., Shisanya, C. A., Mucheru-Muna, M., & Mugendi, D. N.:
1132 Soil greenhouse gas fluxes from maize production under different soil fertility management
1133 practices in East Africa, J. Geophys. Res.: Biogeosciences, 125(7), e2019JG005427,
1134 https://doi.org/10.1029/2019JG005427, 2020.

1135 Malou, O. P., Moulin, P., Chevallier, T., Masse, D., Vayssières, J., Badiane-Ndour, N. Y., Tall, L., Thiam,
1136 A., & Chapuis-Lardy, L.: Estimates of carbon stocks in sandy soils cultivated under local

1137 management practices in Senegal's groundnut basin, Reg. Environ. Change, 21(3), 65,
1138 https://doi.org/10.1007/s10113-021-01790-2, 2021.

1139 Manzoni, S., Chakrawal, A., Fischer, T., Schimel, J. P., Porporato, A., & Vico, G.: Rainfall
1140 intensification increases the contribution of rewetting pulses to soil heterotrophic respiration,
1141 Biogeosciences, 17(15), 4007-4023, https://doi.org/10.5194/bg-17-4007-2020, 2020.

1142 Mapanda, F., Mupini, J., Wuta, M., Nyamangara, J., & Rees, R. M.: A cross-ecosystem assessment of
1143 the effects of land cover and land use on soil emission of selected greenhouse gases and related
1144 soil properties in Zimbabwe, Eur. J. Soil Sci., 61(5), 721-733, https://doi.org/10.1111/j.1365-
1145 2389.2010.01266.x, 2010.

1146 Mazza, G., Agnelli, A. E., & Lagomarsino, A.: The effect of tree species composition on soil C and N
1147 pools and greenhouse gas fluxes in a Mediterranean reforestation, J. Soil Sci. Plant Nutr., 21(2),
1148 1339-1352, https://doi.org/10.1007/s42729-021-00444-w, 2021.

1149 Mbow, C., Van Noordwijk, M., Luedeling, E., Neufeldt, H., Minang, P. A., & Kowero, G.: Agroforestry
1150 solutions to address food security and climate change challenges in Africa, Curr. Opin. Environ.
1151 Sustain., 6(1), 61-67, https://doi.org/10.1016/j.cosust.2013.10.014, 2014.

1152 Meena, A., Hanief, M., Dinakaran, J., & Rao, K. S.: Soil moisture controls the spatio-temporal pattern
1153 of soil respiration under different land use systems in a semi-arid ecosystem of Delhi, India, Ecol.
1154 Processes, 9(1), 15, https://doi.org/10.1186/s13717-020-0218-0, 2020.

1155 Meisner, A., Rousk, J., & Bååth, E.: Prolonged drought changes the bacterial growth response to
1156 rewetting, Soil Biol. Biochem., 88, 314-322, https://doi.org/10.1016/j.soilbio.2015.06.002, 2015.

1157 Merbold, L., Ardo, J., Arneth, A., Scholes, R. J., Nouvellon, Y., de Grandcourt, A., Archibald, S.,
1158 Bonnefond, J. M., Boulain, N., Brueggemann, N., Bruemmer, C., Cappelaere, B., Ceschia, E., El-Khidir,
1159 H. A. M., El-Tahir, B. A., Falk, U., Lloyd, J., Kergoat, L., Le Dantec, V. L., Mougin, E., Muchinda, M.,
1160 Mukelabai, M. M., Ramier, D., Roupsard, O., Timouk, F., Veenendaal, E. M., & Kutsch, W. L.:
1161 Precipitation as driver of carbon fluxes in 11 African ecosystems, Biogeosciences, 6:1027-1041,
1162 https://doi.org/10.5194/bg-6-1027-2009, 2009.

1163 Moncrieff, J., Clement, R., Finnigan, J., Meyers, T.: Averaging, Detrending, and Filtering of Eddy
1164 Covariance Time Series. In: Lee, X., Massman, W., Law, B. (eds) Handbook of Micrometeorology,
1165 Atmos. Ocean. Sci. Lib., vol 29, Springer, Dordrecht, https://doi.org/10.1007/1-4020-2265-4_2,
1166 2004.

1167 Moncrieff, J. B., Massheder, J. M., De Bruin, H., Elbers, J., Friborg, T., Heusinkveld, B., Kabat, P., Scott,
1168 S., Soegaard, H., Verhoef, A.: A system to measure surface fluxes of momentum, sensible heat, water
1169 vapour and carbon dioxide, J. Hydrol., 188, 589-611, https://doi.org/10.1016/S0022-
1170 1694(96)03194-0, 1997.

1171 Mosongo, P. S., Pelster, D. E., Li, X., Gaudel, G., Wang, Y., Chen, S., Li, W., Mburu, D., & Hu, C.:
1172 Greenhouse Gas Emissions Response to Fertilizer Application and Soil Moisture in Dry
1173 Agricultural Uplands of Central Kenya, Atmosphere, 13(3), 463,
1174 https://doi.org/10.3390/atmos13030463, 2022.

1175 Muggeo, V.M.R.: Estimating regression models with unknown break-points. Statist. Med., 22:
1176 3055-3071, https://doi.org/10.1002/sim.1545, 2003.

1177 Munjonji, L., Ntuli Innocentia, H., Ayisi, K. K., Dlamini, P., Mabitsela, K. E., Lehutjo, C. M., &
1178 Magnificent Zwane, P. S.: Seasonal dynamics of soil CO_2 emissions from different semi-arid land-
1179 use systems, Acta. Agr. Scand., Section BSP, 74(1), 2312934,
1180 https://doi.org/10.1080/09064710.2024.2312934, 2024.

1181 Nickerson, N. R.: Evaluating gas emission measurements using Minimum Detectable Flux (MDF),
1182 Eosene White papers, https://eosense.com/wp-content/uploads/2019/11/Eosense-white-
1183 paper-Minimum-Detectable-Flux.pdf, 2016.

1184 Owusu-Prempeh, N., Amekudzi, L. K., & Kyereh, B.: Assessment of soil carbon dioxide efflux from
1185 contrasting land uses in a semi-arid savannah ecosystem, northeastern Ghana (West Africa), Sci.
1186 Afr., 26, e02420, https://doi.org/10.1016/j.sciaf.2024.e02420, 2024.

1187 Oyonarte, C., Rey, A., Raimundo, J., Miralles, I., & Escribano, P.: The use of soil respiration as an
1188 ecological indicator in arid ecosystems of the SE of Spain: Spatial variability and controlling
1189 factors, Ecol. Indic., 14(1), 40-49, https://doi.org/10.1016/j.ecolind.2011.08.013, 2012.

1190 Padfield, D., Matheso, G., & Windram, F.: Package 'Nls. Multstart : Robust Non-Linear Regression
1191 using AIC Scores (R package version 2.0.0), DOI:10.32614/CRAN.package.nls.multstart,
1192 https://cran.r-project.org/web/packages/nls.multstart/nls.multstart.pdf, 2025.

1193 Pelster, D., Rufino, M., Rosenstock, T., Mango, J., Saiz, G., Diaz-Pines, E., Baldi, G., & Butterbach-Bahl,
1194 K., Smallholder farms in eastern African tropical highlands have low soil greenhouse gas fluxes,
1195 Biogeosciences, 14(1), 187-202, https://doi.org/10.5194/bg-14-187-2017, 2017.

Picarro Inc.: PICARRO G2508 CRDS Analyzer N_2O + CH_4 + CO_2 + NH_3 + H_2O in Air, [Datasheet], https://www.picarro.com/sites/default/files/product_documents/Picarro_G2508%20Analyzer%20Datasheet.pdf, 2015.

Placella, S. A., Brodie, E. L., & Firestone, M. K.: Rainfall-induced carbon dioxide pulses result from sequential resuscitation of phylogenetically clustered microbial groups, Proc. Natl. Acad. Sci., 109(27), 10931-10936, https://doi.org/10.1073/pnas.1204306109, 2012.

Pontailler, J. Y., Hymus, G. J., & Drake, B. G.: Estimation of leaf area index using ground-based remote sensed NDVI measurements: Validation and comparison with two indirect techniques, Can. J. Remote Sens., 29(3), 381-387, https://doi.org/10.5589/m03-009, 2003.

Poyda, A., Reinsch, T., Skinner, R. H., Kluß, C., Loges, R., & Taube, F.: Comparing chamber and eddy covariance based net ecosystem CO_2 exchange of fen soils; J. Plant Nutr. Soil Sci., 180(2), 252-266, https://doi.org/10.1002/jpln.201600447, 2017.

Qiu, R., Han, G., Li, S., Tian, F., Ma, X., & Gong, W.: Soil moisture dominates the variation of gross primary productivity during hot drought in drylands, Sci. Total Environ., 899, 165686, https://doi.org/10.1016/j.scitotenv.2023.165686, 2023.

Quansah, E., Mauder, M., Balogun, A. A., Amekudzi, L. K., Hingerl, L., Bliefernicht, J., & Kunstmann, H.: Carbon dioxide fluxes from contrasting ecosystems in the Sudanian Savanna in West Africa, Carbon Balance Manag., 10(1), 1. https://doi.org/10.1186/s13021-014-0011-4, 2015.

Rabbi, S. M. F., Warren, C., Swarbrick, B., Minasny, B., Mcbratney, A., & Young, I.: Microbial decomposition of organic matter and wetting–drying promotes aggregation in artificial soil but porosity increases only in wet-dry condition, Geoderma, 447, 116924, https://doi.org/10.1016/j.geoderma.2024.116924, 2024.

Rahimi, J., Ago, E. E., Ayantunde, A., Berger, S., Bogaert, J., Butterbach-Bahl, K., Cappelaere, B., Cohard, J.-M., Demarty, J., Diouf, A. A., Falk, U., Haas, E., Hiernaux, P., Kraus, D., Roupsard, O., Scheer, C., Srivastava, A. K., Tagesson, T., & Grote, R.: Modeling gas exchange and biomass production in West African Sahelian and Sudanian ecological zones, Geosci. Model Dev., 14(6), 3789-3812, https://doi.org/10.5194/gmd-14-3789-2021, 2021.

Raich, J. W., Lambers, H., & Oliver, D. J.: Respiration in Terrestrial Ecosystems, In D. M. Karl, & W. H., Schlesinger (Eds.), Treatise Geochem., (2 ed., Vol. 10, pp. 613-649), Elsevier, https://doi.org/10.1016/B978-0-08-095975-7.00817-2, 2014.

Ramesh, T., Manjaiah, K. M., Tomar, J. M. S., & Ngachan, S. V.: Effect of multipurpose tree species on soil fertility and CO_2 efflux under hilly ecosystems of Northeast India, Agr. Syst., 87(6), 1377-1388, https://doi.org/10.1007/s10457-013-9645-6, 2013.

R. Core Team.: R: A language and environment for statistical computing, R Foundation for Statistical Computing, Vienna, Austria, 2023.

Reichle, D. E.: Energy flow in ecosystems., In D.E. Reichle (ed) The Global Carbon Cycle and Climate Change (p. 119-156), Elsevier, https://doi.org/10.1016/B978-0-12-820244-9.00008-1, (2020).

Reichstein, M., et al.: Modeling temporal and large-scale spatial variability of soil respiration from soil water availability, temperature and vegetation productivity indices, Global Biogeochem. Cycles, 17, 1104, doi:10.1029/2003GB002035, 4, 2003.

Reichstein, M., Falge, E., Baldocchi, D., Papale, D., Aubinet, M., Berbigier, P., Bernhofer, C., Buchmann, N., Gilmanov, T., Granier, A., Grünwald, T., Havránková, K., Ilvesniemi, H., Janous, D., Knohl, A., Laurila, T., Lohila, A., Loustau, D., Matteucci, G., … Valentini, R.: On the separation of net ecosystem exchange into assimilation and ecosystem respiration: Review and improved algorithm, Glob. Change Biol., 11(9), 1424-1439, https://doi.org/10.1111/j.1365-2486.2005.001002.x, 2005.

Reum, F., Gerbig, C., Lavric, J. V., Rella, C. W., & Göckede, M.: Correcting atmospheric CO_2 and CH_4 mole fractions obtained with Picarro analyzers for sensitivity of cavity pressure to water vapor, Atmos. Meas. Tech., 12(2), 1013-1027, https://doi.org/10.5194/amt-12-1013-2019, 2005.

Rheault, K., Riis Christiansen, J., & Steenberg Larsen, K.: The role of tree species and microbes for the development of net greenhouse gas fluxes from soils after afforestation of agricultural lands, EGU General Assembly 2024, Vienna, Austria, 14-19 April 2024, EGU24-9718, https://doi.org/10.5194/egusphere-egu24-9718, 2024.

Richardson, J., Chatterjee, A., & Darrel Jenerette, G.: Optimum temperatures for soil respiration along a semi-arid elevation gradient in southern California, Soil Biol. Biochem., 46, 89-95, https://doi.org/10.1016/j.soilbio.2011.11.008, 2012.

Riederer, M., Serafimovich, A., & Foken, T.: Net ecosystem CO_2 exchange measurements by the closed chamber method and the eddy covariance technique and their dependence on atmospheric conditions, Atmos. Meas. Tech., 7(4), 1057-1064, https://doi.org/10.5194/amt-7-1057-2014, 2014.

1256 Roby, M. C., Scott, R. L., Biederman, J. A., Smith, W. K., & Moore, D. J. P.: Response of soil carbon
1257 dioxide efflux to temporal repackaging of rainfall into fewer, larger events in a semiarid grassland,
1258 Front. Environ. Sci., 10. https://doi.org/10.3389/fenvs.2022.940943, 2022.

1259 Rolo, V., Rivest, D., Maillard, É., & Moreno, G.: Agroforestry potential for adaptation to climate
1260 change: A soil-based perspective, Soil Use Manag., 39(3), 1006-1032,
1261 https://doi.org/10.1111/sum.12932, 2023.

1262 Rong, Y., Ma, L., Johnson, D., & Yuan, F.: Soil respiration patterns for four major land-use types of
1263 the agro-pastoral region of northern China, Agr. Ecosyst Environ., 213, 142-150,
1264 https://doi.org/10.1016/j.agee.2015.08.002, 2015.

1265 Rosenstock, T. S., Mpanda, M., Pelster, D. E., Butterbach-Bahl, K., Rufino, M. C., Thiong'o, M., Mutuo,
1266 P., Abwanda, S., Rioux, J., Kimaro, A. A., & Neufeldt, H.: Greenhouse gas fluxes from agricultural
1267 soils of Kenya and Tanzania: GHG Fluxes From Agricultural Soils of East Africa, J. Geophys. Res.:
1268 Biogeosciences, 121(6), 1568-1580, https://doi.org/10.1002/2016JG003341, 2016.

1269 Roupsard, O., Ferhi, A., Granier, A., Pallo, F., Depommier, D., Mallet, B., Joly, H. I., & Dreyer, E.:
1270 Reverse Phenology and Dry-Season Water Uptake by *Faidherbia albida* (Del.) A. Chev. in an
1271 Agroforestry Parkland of Sudanese West Africa, Funct. Ecol., 13(4), 460–472,
1272 http://www.jstor.org/stable/2656552, 1999.

1273 Roupsard, O., Audebert, A., Ndour, A. P., Clermont-Dauphin, C., Agbohessou, Y., Sanou, J., Koala, J.,
1274 Faye, E., Sambakhe, D., Jourdan, C., le Maire, G., Tall, L., Sanogo, D., Seghieri, J., Cournac, L., & Leroux,
1275 L.: How far does the tree affect the crop in agroforestry? New spatial analysis methods in a
1276 *Faidherbia* parkland, Agr. Ecosyst. Environ, 296, 106928,
1277 https://doi.org/10.1016/j.agee.2020.106928, 2020.

1278 Sarr, M.S., Diouf D., Roupsard O., Rocheteau A., Orange D., et al.: Estimation of seasonal water use
1279 of *Faidherbia albida* (Delile) A. Chev. in a Sahelian agroforestry parkland, Biotechnol. Agron. Soc.
1280 Environ., 27(3), 196-204, https://doi.org/10.25518/1780-4507.20512., 2023.

1281 Schimel, J., Balser, T. C., & Wallenstein, M.: Microbial stress-response physiology and its
1282 implications for ecosystem function, Ecology, 88(6), 1386-1394, https://doi.org/10.1890/06-
1283 0219, 2007.

1284 Sida, T. S., Baudron, F., Kim, H., & Giller, K. E.: Climate-smart agroforestry: *Faidherbia albida* trees
1285 buffer wheat against climatic extremes in the Central Rift Valley of Ethiopia, Agr. Forest Meteorol.,
1286 248, 339-347, https://doi.org/10.1016/j.agrformet.2017.10.013, 2018.

Siegwart, L., Bertrand, I., Roupsard, O., Duthoit, M., & Jourdan, C.: Root litter decomposition in a sub-Sahelian agroforestry parkland dominated by *Faidherbia albida*, J. Arid Environ., 198, 104696, https://doi.org/10.1016/j.jaridenv.2021.104696, 2022.

Siegwart, L., Bertrand, I., Roupsard, O., & Jourdan, C.: Contribution of tree and crop roots to soil carbon stocks in a Sub-Sahelian agroforestry parkland in Senegal, Agr. Ecosyst. Environ., 352, 108524, https://doi.org/10.1016/j.agee.2023.108524, 2023.

Sileshi, G. W.: The magnitude and spatial extent of influence of *Faidherbia albida* trees on soil properties and primary productivity in drylands, J. Arid Environ., 132, 1-14, https://doi.org/10.1016/j.jaridenv.2016.03.002, 2016.

Sileshi, G. W., Teketay, D., Gebrekirstos, A., & Hadgu, K.: Sustainability of *Faidherbia albida*-Based Agroforestry in Crop Production and Maintaining Soil Health., In J. C. Dagar, S. R. Gupta, & D. Teketay (eds), Agroforestry for Degraded Landscapes: Recent Advances and Emerging Challenges—Vol., 2 (p. 349-369), Springer Singapore, https://doi.org/10.1007/978-981-15-6807-7_12, 2020.

Singh, S., Mayes, M., Kivlin, S., & Jagadamma, S.: How the Birch Effect differs in mechanisms and magnitudes due to soil texture, Soil Biol. Biochem., 179, 108973, https://doi.org/10.1016/j.soilbio.2023.108973, 2023.

Soudani, K., Hmimina, G., Delpierre, N., Pontailler, J. Y., Aubinet, M., Bonal, D., Caquet, B., de Grandcourt, A., Burban, B., Flechard, C., Guyon, D., Granier, A., Gross, P., Heinesh, B., Longdoz, B., Loustau, D., Moureaux, C., Ourcival, J. M., Rambal, S., Saint André.L, Dufrene, E.: Ground-based Network of NDVI measurements for tracking temporal dynamics of canopy structure and vegetation phenology in different biomes, Remote Sens. Environ., 123, 234-245, https://doi.org/10.1016/j.rse.2012.03.012, 2012.

Skinner, R. H., & Wagner-Riddle, C.: Micrometeorological Methods for Assessing Greenhouse Gas Flux., In M. A. Liebig, A. J. Franzluebbers, & R. F. Follett (eds) Managing Agricultural Greenhouse Gases: Coordinated Agricultural Research through GRACEnet to Address our Changing Climate (p. 367-383), Elsevier, https://doi.org/10.1016/B978-0-12-386897-8.00021-8, 2012.

Stephen, E. A., Evans, K. D., & Akwasi, A. A.: Effects of *Faidherbia albida* on some important soil fertility indicators on agroforestry parklands in the semi-arid zone of Ghana, Afr. J. Agr. Res., 15(2), 256-268, https://doi.org/10.5897/ajar2019.14617, 2020.

Stetter, C., & Sauer, J.: Tackling climate change: Agroforestry adoption in the face of regional weather extremes, Ecol. Econ., 224, 108266, https://doi.org/10.1016/j.ecolecon.2024.108266, 2024.

Stojanović, M., Jocher, G., Kowalska, N., Szatniewska, J., Zavadilová, I., Urban, O., Čáslavský, J., Horáček, P., Acosta, M., Pavelka, M., & Marshall, J. D.: Disaggregation of canopy photosynthesis among tree species in a mixed broadleaf forest, Tree Physiol., 44(7), tpae064, https://doi.org/10.1093/treephys/tpae064, 2024.

Tagesson, T., Ardö, J., Guiro, I., Cropley, F., Mbow, C., Horion, S., Ehammer, A., Mougin, E., Delon, C., Galy-Lacaux, C., & Fensholt, R.: Very high CO_2 exchange fluxes at the peak of the rainy season in a West African grazed semi-arid savanna ecosystem, Geografisk Tidsskrift – Dan. J. of Geogr., 116(a), 93-109, https://doi.org/10.1080/00167223.2016.1178072, 2016.

Tagesson, T., Fensholt, R., Cappelaere, B., Mougin, E., Horion, S., Kergoat, L., Nieto, H., Mbow, C., Ehammer, A., Demarty, J., & Ardö, J.: Spatiotemporal variability in carbon exchange fluxes across the Sahel, Agr. Forest Meteorol., 226-227(b), 108-118, https://doi.org/10.1016/j.agrformet.2016.05.013, 2016.

Tagesson, T., Fensholt, R., Cropley, F., Guiro, I., Horion, S., Ehammer, A., & Ardö, J.: Dynamics in carbon exchange fluxes for a grazed semi-arid savanna ecosystem in West Africa. Agr. Ecosyst. Environ., 205, 15-24, https://doi.org/10.1016/j.agee.2015.02.017, 2015.

Tang, J., Bolstad, P. V., Desai, A. R., Martin, J. G., Cook, B. D., Davis, K. J., & Carey, E. V.: Ecosystem respiration and its components in an old-growth forest in the Great Lakes region of the United States, Agr. Forest Meteorol., 148(2), 171-185, https://doi.org/10.1016/j.agrformet.2007.08.008, 2008.

Tang, X., Carvalhais, N., Moura, C., Ahrens, B., Koirala, S., Fan, S., Guan, F., Zhang, W., Gao, S., Magliulo, V., Buysse, P., Liu, S., Chen, G., Yang, W., Yu, Z., Liang, J., Shi, L., Pu, S., & Reichstein, M.: Global variability of carbon use efficiency in terrestrial ecosystems, Biogeochemistry: Land, https://doi.org/10.5194/bg-2019-37, 2019.

Tucker, C. L., & Reed, S. C.: Low soil moisture during hot periods drives apparent negative temperature sensitivity of soil respiration in a dryland ecosystem: A multi-model comparison, Biogeochemistry, 128(1-2), 155-169, https://doi.org/10.1007/s10533-016-0200-1, 2016.

Unger, S., Máguas, C., Pereira, J. S., David, T. S., & Werner, C.: The influence of precipitation pulses on soil respiration – Assessing the "Birch effect" by stable carbon isotopes, Soil Biol. Biochem., 42(10), 1800-1810, https://doi.org/10.1016/j.soilbio.2010.06.019, 2010.

Valujeva, K., Pilecka-Ulcugaceva, J., Skiste, O., Liepa, S., Lagzdins, A., & Grinfelde, I.: Soil tillage and agricultural crops affect greenhouse gas emissions from Cambic Calcisol in a temperate climate, Acta. Agr. Scand. B-S-P., 72(1), 835-846, https://doi.org/10.1080/09064710.2022.2097123, 2022.

Van Haren, J. L. M., De Oliveira, R. C., Restrepo-Coupe, N., Hutyra, L., De Camargo, P. B., Keller, M., & Saleska, S. R.: Do plant species influence soil CO_2 and N_2 O fluxes in a diverse tropical forest? J. Geophys. Res.: Biogeosciences, 115, G03010, https://doi.org/10.1029/2009JG001231, 2010.

Vargas, R., Enrique, S. C. P., Serrano-Ortiz, P., Yuste, J. C., Domingo, F., López-Ballesteros, A., & Oyonarte, C.: Hot-moments of soil CO_2 efflux in a water-limited grassland, Soil Syst., 2(3), 1-18, https://doi.org/10.3390/soilsystems2030047, 2018.

Vickers, D., & Mahrt, L.: Quality Control and Flux Sampling Problems for Tower and Aircraft Data, J. Atmos. Oceanic Technol., 14(3), 512-526, http://dx.doi.org/10.1175/1520-0426(1997)014%3C0512:QCAFSP%3E2.0.CO;2, 1997.

Wachiye, S., Merbold, L., Vesala, T., Rinne, J., Räsänen, M., Leitner, S., & Pellikka, P.: Soil greenhouse gas emissions under different land-use types in savanna ecosystems of Kenya, Biogeosciences, 17(8), 2149-2167, https://doi.org/10.5194/bg-17-2149-2020, 2020.

Wang, M., Guan, D.-X., Han, S.-J., & Wu, J.-L.: Comparison of eddy covariance and chamber-based methods for measuring CO_2 flux in a temperate mixed forest, Tree Physiol., 30(1), 149-163, https://doi.org/10.1093/treephys/tpp098, 2010.

Wang, Z., Ji, L., Hou, X., & Schellenberg, M. P.: Soil Respiration in Semiarid Temperate Grasslands under Various Land Management, PLOS ONE, 11(1), e0147987, https://doi.org/10.1371/journal.pone.0147987, 2016.

Waring E., Quinn M., McNamara A., Arino de la Rubia E., Zhu H., Ellis S.: skimr: Compact and Flexible Summaries of Data, R package (version 2.1.5), https://github.com/ropensci/skimr/, https://docs.ropensci.org/skimr/ (website), 2024.

Warren, C. R. Response of osmolytes in soil to drying and rewetting. Soil Biol. Biochem., 70, 22-32, https://doi.org/10.1016/j.soilbio.2013.12.008, 2014.

Webb, E. K., Pearman, G. I., & Leuning, R., Correction of flux measurements for density effects due to heat and water vapour transfer. Q. J. R. Meteorol. Soc., 106, 85-100, https://doi.org/10.1002/qj.49710644707, 1980.

Wieckowski, A., Vestin, P., Ardö, J., Roupsard, O., Ndiaye, O., Diatta, O., Ba, S., Agbohessou, Y., Fensholt, R., Verbruggen, W., Gebremedhn, H. H., & Tagesson, T.: Eddy covariance measurements reveal a decreased carbon sequestration strength 2010–2022 in an African semiarid savanna, Glob. Change Biol., 30(9), e17509. https://doi.org/10.1111/gcb.17509, 2024.

Wiesner, S., Desai, A. R., Duff, A. J., Metzger, S., & Stoy, P. C.: Quantifying the natural climate solution potential of agricultural systems by combining eddy covariance and remote sensing. J. Geophys. Res.: Biogeosciences, 127(9), e2022JG006895, https://doi.org/10.1029/2022JG006895, 2022.

Wild, J., Kopecký, M., Macek, M., Šanda, M., Jankovec, J., & Haase, T.: Climate at ecologically relevant scales: A new temperature and soil moisture logger for long-term microclimate measurement, Agr. Forest Meteorol., 268, 40-47, https://doi.org/10.1016/j.agrformet.2018.12.018, 2019.

Williams, C.A., Hanan, N.P., Neff, J.C. et al.: Africa and the global carbon cycle, Carbon Balance Manage., 2, 3, https://doi.org/10.1186/1750-0680-2-3, 2007.

Williams, C. A., Hanan, N., Scholes, R. J., & Kutsch, W.: Complexity in water and carbon dioxide fluxes following rain pulses in an African savanna, Oecologia, 161(3), 469-480, https://doi.org/10.1007/s00442-009-1405-y, 2009.

Wohlfahrt, G., & Galvagno, M.: Revisiting the choice of the driving temperature for eddy covariance CO_2 flux partitioning, Agr. Forest Meteorol., 237-238, 135-142, https://doi.org/10.1016/j.agrformet.2017.02.012, 2017.

Wutzler, T., Lucas-Moffat, A., Migliavacca, M., Knauer, J., Sickel, K., Šigut, L., Menzer, O., and Reichstein, M.: Basic and extensible post-processing of eddy covariance flux data with REddyProc, Biogeosciences, 15, 5015–5030, https://doi.org/10.5194/bg-15-5015-2018, 2018.

Xenakis, G.: FREddyPro: Post-Processing EddyPro Full Output File. Edinburgh, UK. R package version 1.0.1., 2016.

Xue, H., & Tang, H.: Responses of soil respiration to soil management changes in an agropastoral ecotone in Inner Mongolia, China, Ecol. Evol., 8(1), 220-230, https://doi.org/10.1002/ece3.3659, 2018.

Yan, L., Chen, S., Xia, J., & Luo, Y.: Precipitation regime shift enhanced the rain pulse effect on soil respiration in a semi-arid steppe, PLoS ONE, 9(8), https://doi.org/10.1371/journal.pone.0104217, 2014.

Yu, H., Xu, Z., Zhou, G., & Shi, Y.: Soil carbon release responses to long-term versus short-term climatic warming in an arid ecosystem, Biogeosciences, 17(3), 781-792, https://doi.org/10.5194/bg-17-781-2020, 2020.

Yu, T., Jiapaer, G., Bao, A., Zheng, G., Zhang, J., Li, X., Yuan, Y., Huang, X., & Umuhoza, J.: Disentangling the relative effects of soil moisture and vapor pressure deficit on photosynthesis in dryland Central Asia, Ecol. Indic., 137, 108698, https://doi.org/10.1016/j.ecolind.2022.108698, 2022.

Yu, X., Zha, T., Pang, Z., Wu, B., Wang, X., Chen, G., Li, C., Cao, J., Jia, G., Li, X., & Wu, H.: Response of soil respiration to soil temperature and moisture in a 50-year-old oriental arborvitae plantation in China, PLoS ONE, 6(12), https://doi.org/10.1371/journal.pone.0028397, 2011.

Zaman M., Kleineidam K., Bakken L., Berendt J., Bracken C., Butterbach-Bahl K., Cai Z., Chang S. X., Clough T., Dawar K., Ding W. X., Dörsch P., dos Reis Martins M., Eckhardt C., Fiedler S., Frosch T., Goopy J., Görres C.-M., Gupta A., Henjes S., Hofmann M. E. G., Horn M. A,. Jahangir M. M. R., Jansen-Willems A., Lenhart K., Heng L., Lewicka-Szczebak D., Lucic G., Merbold L., Mohn J., Molstad L., Moser G., Murphy P., Sanz-Cobena A., Šimek M., Urquiaga S., Well R., Wrage-Mönnig N., Zaman S., Zhang J., Müller C.: Greenhouse Gases from Agriculture. In M. Zaman, L. Hang, C. Müller (eds) Measuring emission of agricultural greenhouse gases and developing mitigation options using nuclear and related techniques Springer, Cham, https://doi.org/10.1007/978-3-030-55396-8_1, 2021.

Zeileis, A., Grothendieck, G., Ryan, J. A., Ulrich, J. M., & Andrews, F.: Package 'zoo': S3 Infrastructure for Regular and Irregular Time Series (Z's Ordered Observations) (version 1.8-12) [R Package], https://zoo.R-Forge.R-project.org/, 2024.

Zhang, X., Bi, J., Zhu, D., & Meng, Z.: Seasonal variation of net ecosystem carbon exchange and gross primary production over a Loess Plateau semi-arid grassland of northwest China, Sci. Rep. 14(1), 2916, https://doi.org/10.1038/s41598-024-52559-6, 2024.

Zhang, X., Ramakanth, K. K., & Long, Y.: The biomechanics of turgor pressure, Curr. Biol., 34(20), R986-R991, https://doi.org/10.1016/j.cub.2024.07.013, 2024.

Zhao, C., Miao, Y., Yu, C., Zhu, L., Wang, F., Jiang, L., Hui, D., & Wan, S.: Soil microbial community composition and respiration along an experimental precipitation gradient in a semiarid steppe, Sci. Rep., 6(1), 24317, https://doi.org/10.1038/srep24317, 2016.

Zhou, Y., Williams, C. A., Lauvaux, T., Feng, S., Baker, I. T., Wei, Y., Denning, A. S., Keller, K., & Davis, K. J.: ACT-America: Gridded Ensembles of Surface Biogenic Carbon Fluxes, 2003-2019 (Version 1.1), ORNL Distributed Active Archive Center, https://doi.org/10.3334/ORNLDAAC/1675, 2019.

Zhou, Y., Williams, C. A., Lauvaux, T., Davis, K. J., Feng, S., Baker, I., et al.: A multiyear gridded data ensemble of surface biogenic carbon fluxes for North America: Evaluation and analysis of results, J. Geophys. Res.: Biogeosciences, 125, e2019JG005314, https://doi.org/10.1029/2019JG005314, 2020.